

Supporting information for

Dithia[9]helicenes: Molecular Design, Surface Imaging, and Circularly Polarized Luminescence with Enhanced Dissymmetry Factors

Bianca C. Baciú,^a Pawel J. Bronk,^a Tamara de Ara,^b Rafael Rodriguez,^c Pierpaolo Morgante,^e Nicolas Vanthuyne,^d Carlos Sabater,^b Carlos Untiedt,^b Jochen Autschbach^{*,e} Jeanne Crassous,^{*,c} Albert Guijarro.^{*,a}

^a *Departamento de Química Orgánica and Instituto Universitario de Síntesis Orgánica, Unidad asociada CSIC, Universidad de Alicante, Campus de San Vicente del Raspeig, E-03080, Alicante, Spain*

^b *Departamento de Física Aplicada and Unidad asociada CSIC, Universidad de Alicante, Campus de San Vicente del Raspeig, E-03080, Alicante, Spain*

^c *Université Rennes, CNRS, ISCR-UMR 6226, Rennes F-35000, France*

^d *Aix Marseille University, CNRS, Centrale Marseille, iSm2, Marseille, France*

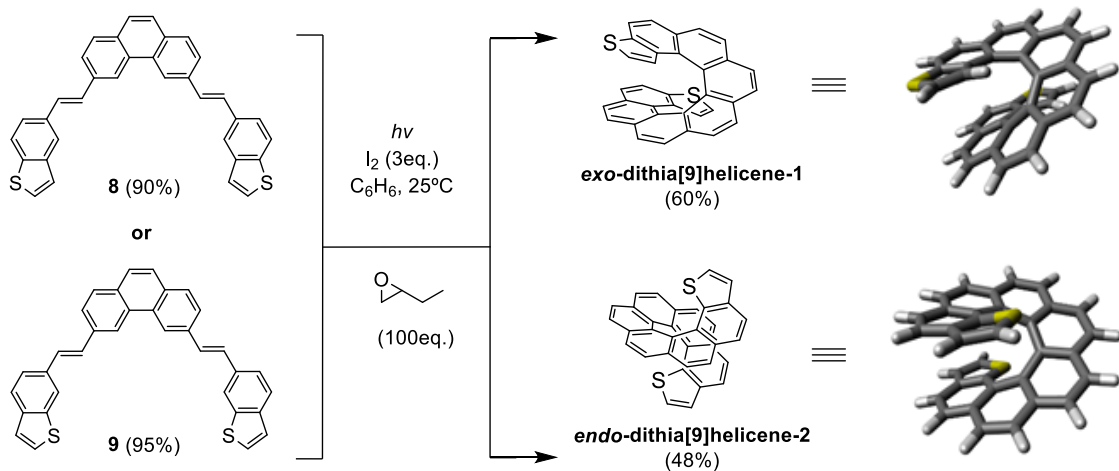
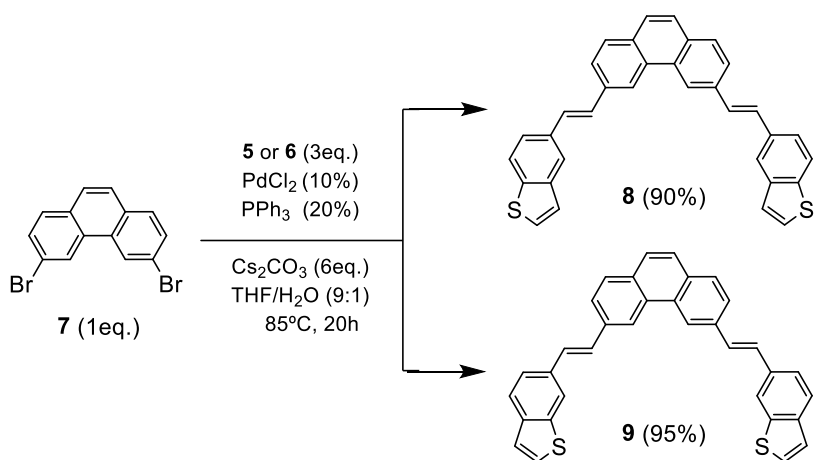
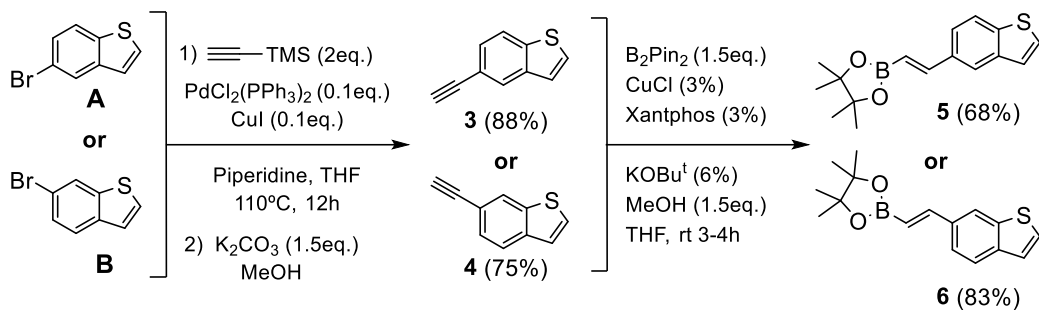
^e *Department of Chemistry, University at Buffalo, State University of New York, Buffalo, New York 14260, United States*

Table of Contents

Section S1: Experimental part	3
1. Synthesis of <i>exo</i>-dithia[9]helicene and <i>endo</i>-dithia[9]helicene	3
2. General Methods	4
3. Photochemistry	5
4. Synthesis and characterization of compounds	5
4.1. 5-Ethynylbenzo[<i>b</i>]thiophene (3)	5
4.2. (<i>E</i>)-2-(2-(Benzo[<i>b</i>]thiophen-5-yl)vinyl)-4,4,5,5-tetramethyl-1,3,2-dioxaborolane (5)	6
4.3. 3,6-Bis((<i>E</i>)-2-(benzo[<i>b</i>]thiophen-5-yl)vinyl)phenanthrene (8)	7
4.4. <i>Exo</i> -dithia[9]helicene (1).....	7
5. ¹H NMR and ¹³C NMR spectra of compounds	9
5.1. 5-Ethynylbenzo[<i>b</i>]thiophene (300MHz, CDCl ₃).....	9
5.2. 6-Ethynylbenzo[<i>b</i>]thiophene (300MHz, CDCl ₃).....	10
5.3. (<i>E</i>)-2-(2-(Benzo[<i>b</i>]thiophene-5-yl)vinyl)-4,4,5,5-tetramethyl-1,3,2-dioxaborolane (300MHz, CDCl ₃).....	11
5.4. (<i>E</i>)-2-(2-(Benzo[<i>b</i>]thiophene-6-yl)vinyl)-4,4,5,5-tetramethyl-1,3,2-dioxaborolane (300MHz, CDCl ₃).....	12
5.5. 3,6-Bis((<i>E</i>)-2-(benzo[<i>b</i>]thiophen-5-yl)vinyl)phenanthrene (400MHz, CDCl ₃)	13
5.6. 3,6-Bis((<i>E</i>)-2-(benzo[<i>b</i>]thiophen-6-yl)vinyl)phenanthrene (300MHz, CDCl ₃)	13
5.7. <i>Exo</i> -dithia[9]helicene (400MHz, Methylene chloride- <i>d</i> ₂)	14
5.8. <i>Endo</i> -dithia[9]helicene (300MHz, CDCl ₃).....	15
6. HMRS (ESI)	16
7. X-ray diffraction (XRD) analysis	17
8. List of possible isomeric structures in the synthesis of <i>exo</i>-1 and <i>endo</i>-2	21
9. HPLC separations	21
10. Photophysical and chiroptical studies	28
10.1. CD and CPL measurements	28
11. Scanning Tunneling Microscopy (STM)	29
Section S2: Theoretical part	30
1. Computational details.	30
2. Optimized structures in Cartesian coordinates (xyz format).	51
3. Additional structures optimized with ωB97X-D/def2-SV(P).	62
Section S3: Additional references.	65

Section S1: Experimental part

1. Synthesis of *exo*-dithia[9]helicene and *endo*-dithia[9]helicene



2. General Methods

Commercially starting materials and solvents for photochemistry, chromatography and recrystallization were used without further purification, unless otherwise stated. THF, benzene and cyclohexane were dried and distilled over Na/K alloy right before. Commercially unavailable reagents were synthesized via different methods that will be explained separately.

Gas chromatography analyses (GLC) were carried out with a Hewlett Packard HP-5890 instrument equipped with a flame ionization detector and a 30 m HP-5 capillary column (0.32 mm diam, 0.25 μm film thickness), using nitrogen as carrier gas (12 psi). Column chromatography was performed with Merck silica gel 60 (0.040-0.063 μm , 240-400 mesh). Thin-layer chromatography (TLC) was performed on precoated silica gel plates (Merck 60, F254, 0.25 mm). TLC detection was done by UV₂₅₄ light, R_f values are given under these conditions. NMR spectra were recorded on a Bruker Avance 300 and Bruker Avance 400 (300 and 400 MHz for ¹H-NMR, and 75 and 100 MHz for ¹³C-NMR respectively) using CDCl₃ as a solvent and TMS as internal standard. Chemical shifts (δ) are given in ppm vs. TMS. Infrared (IR) analysis was performed with a JASCO FT/IR 4100 spectrophotometer equipped with an ATR component. LRMS were performed using the electron impact (EI) mode at 70 eV in an AGILENT 5973N mass spectrometer coupled with an AGILENT 6890N gas chromatographer. Melting points were performed with a Reichert Thermovar polarizing light microscope and melting points apparatus and have been corrected. Differential scanning calorimetry (DSC) analyses were performed with a calorimeter of TA INSTRUMENTS model Q100 mDSC.

Absorption spectra of UV-Visible (UV-vis, in $\text{M}^{-1} \text{cm}^{-1}$) were recorded on a UV-2401PC Shimadzu spectrophotometer. Fluorescence spectra were recorded on a FL 920 Edinburgh fluorimeter. Fluorescence quantum yields ϕ were measured in diluted solutions using the following equation:

$$\phi_X = \phi_{ST} \left(\frac{\text{Grad}_X}{\text{Grad}_{ST}} \right) \left(\frac{\eta^2_X}{\eta^2_{ST}} \right)$$

The parameters that appear in the equation mean: the subscripts ST and X denote standard and sample respectively, ϕ is the fluorescence quantum yield, Grad is the gradient from the plot of integrated fluorescence intensity vs absorbance, and η the refractive index of the solvent. Quantum yield measurements were carried out using quinine in sulfuric acid as reference (excitation of reference and sample compounds was performed at the same wavelength). Spectra were recorded in CH₂Cl₂ at room temperature and in 1-methyl-THF (Me-THF) at 77 K. Optical Rotations were measured on a Jasco P-200.

Electronic circular dichroism (ECD, in $\text{M}^{-1} \text{cm}^{-1}$) was measured on a Jasco J-815 Circular dichroism Spectrometer (IFR140 facility- Biosit- Université de Rennes 1). The circularly polarized luminescence (CPL) measurements were performed using a home-built CPL spectrofluoropolarimeter (constructed with the help of the JASCO Company). The samples were excited using a 90° geometry with a Xenon ozone-free lamp 150 W LS. The concentration of the sample was ca. 10^{-5} M. Spectra were recorded in CH₂Cl₂ with 10 accumulations.

3. Photochemistry

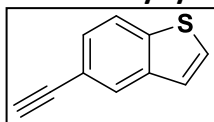
Two different photochemical setups (400 W high-pressure Hg lamps and 2×50 W, 365 nm LED board) were used for the final Mallory-Katz photocyclizations reaction.

A 400-watt high-pressure mercury lamp (Osram HQL MBF-U) was modified by cutting away the outer glass envelope from the screw base (preserving the inner quartz arc tube containing Hg) and was mounted in a porcelain lamp holder provided with a reflector. The lamp was connected to a corresponding power unit and the light beam was focused horizontally to a number of 100mL Schlenck's tubes provided with magnetic stirring and a vertical condenser ending up with a bubbler and refrigerated with a recirculating chiller. 30% ethylene glycol -water mixture as a coolant. The chemical hood was lined with aluminum foil to avoid unwanted exposure to UV radiation. We used cyclohexane or benzene under reflux as solvents. For the degassed reaction, Ar was mildly bubbled through the reaction mixture using a 2 mm flexible Teflon tube.

Two 50 W LED boards were fixed to the walls of a vertical aluminum cylinder (15 cm diameter × 25 cm height) facing each other on opposite sides and connected to the corresponding power units. Small heat dissipaters provided with fans were attached to the LED boards to prevent overheating. This constituted the irradiation chamber. A 250 mL Schlenk 0.6 mm thick single-walled borosilicate tube was placed in the middle of this chamber containing the reaction mixture and was irradiated from opposite sides, at ca. 4 cm distance from each LED plate, while being magnetically stirred from the bottom. With this setup, we worked without reflux and no additional refrigeration of the central reaction tube was needed. We use cyclohexane or benzene as solvents. For the degassed reaction, Ar was mildly bubbled through the reaction as explained above.

4. Synthesis and characterization of compounds

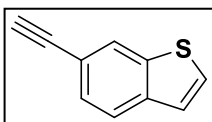
4.1. 5-Ethynylbenzo[b]thiophene (**3**)¹



This compound was prepared by adapting a Sonogashira coupling described in the literature to our substrates¹. A pressure tube was charged with a stirbar, Pd(PPh₃)₂Cl₂ (145.80 mg; 0.2 mmol; 0.1 eq.), CuI (39.71 mg; 0.2 mmol; 0.1 eq.) and 5-bromobenzo[b]thiophene (426.18 mg; 2 mmol; 1eq.).

The tube was sealed with septum and three cycles vacuum/argon were then performed. Then 4.4mL of dry THF and 2.2mL of dry piperidine followed by trimethylsilylacetylene (0.56mL, 4 mmol; 2 eq.) were added via syringe. The tube was closed and heated in an oil bath at 110°C overnight. The reaction was monitored by TLC. After completion, the dark solution was filtered through a pad of celite. The crude product was purified by column chromatography (silica gel, hexane). The combined fractions were evaporated, and the yellow solid was immediately dissolved in MeOH (20mL) and treated with solid K₂CO₃ (418 mg; 3 mmol) with vigorous stirring for 3 hours. The work up consisted in an extraction using 5mL of H₂O and 3×10mL of EtOAc. The organic phase was then dried over magnesium sulfate, filtered and the solvent evaporated under reduced pressure (15 Torr). The residue was purified by column chromatography on silica gel (hexane) to obtain a yellow oil in 88% yield.

Yellow oil; *R*_f=0.44 (hexane); ¹H-NMR (CDCl₃, 300MHz): δ= 7.99 (d, *J*= 1.1 Hz, 1H), 7.83 (d, *J*=8.4 Hz, 1H), 7.51-7.43 (m, 2H), 7.35-7.29 (m, 1H), 3.11 (s, 1H). ¹³C-NMR (CDCl₃, 75 MHz): δ= 140.26, 139.55, 127.71, 127.70, 127.61, 123.75, 122.57, 118.08, 84.08, 76.82. MS (EI) *m/z* 160.05 (M⁺+2, 4.7), 159.10 (M⁺+1, 11.6), 158.10 (M⁺, 100), 114.10 (14.5), 113.10 (6.2), 79.10 (3.9). IR (neat) *v*_{max} 3292.86, 1432.85, 1314.25, 1156.12, 1116.58, 895.77, 824.42, 808.99, 753.10, 732.82, 696.18cm⁻¹.

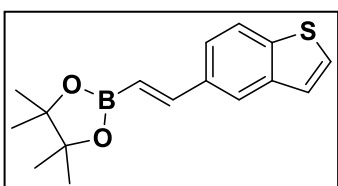


6-Ethynylbenzo[b]thiophene (4)²

This compound was prepared following the previous procedure, but in this case replacing 5-bromobenzo[b]thiophene by 6-bromobenzo[b]thiophene.

Yellow oil in 75% yield; $R_f=0.48$ (hexane); $^1\text{H-NMR}$ (CDCl_3 , 300MHz): $\delta= 8.05$ (s, 1H), 7.77 (d, $J= 8.3$ Hz, 1H), 7.52 (d, $J=5.4$ Hz, 1H), 7.49 (dd, $J= 8.3, 1.4$ Hz, 1H), 7.33 (dd, $J= 5.4, 0.7$ Hz, 1H), 3.14 (s, 1H). $^{13}\text{C-NMR}$ (CDCl_3 , 75 MHz): $\delta= 139.80, 139.62, 128.28, 128.02, 126.57, 123.91, 123.52, 117.99, 84.02, 77.35$. MS (EI) m/z 160.10 (M^{+2} , 5.1), 159.10 (M^{+1} , 12.0), 158.10 (M^+ , 100), 114.10 (13.5), 113.10 (6.3), 79.10 (3.8). IR (neat) ν_{max} 3297.68, 1455.03, 1385.6, 1214.93, 1080.91, 1046.19, 907.34, 823.45, 753.20, 732.78, 697.14. 663.39cm^{-1} .

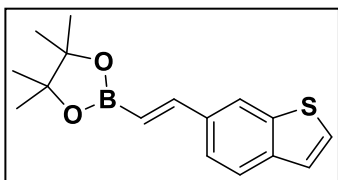
4.2. (E)-2-(2-(Benzo[b]thiophen-5-yl)vinyl)-4,4,5,5-tetramethyl-1,3,2-dioxaborolane (5)³



The compound was prepared by adapting to our substrates a procedure of hydroboration of alkynes⁴. In an oven-dried Schlenk tube, CuCl (8.17 mg; 0.082 mmol; 0.03 eq.), NaOt-Bu (15.86 mg; 0.164 mmol; 0.06 eq.) and Xantphos ligand (47.33 mg; 0.082 mmol; 0.03 eq.) were added. After three cycles of vacuum/argon,

2.5mL of dry THF were injected and the solution was stirred for 30 minutes at room temperature. Then bis(pinacolato)diboron (1.39 g; 5.46 mmol; 2 eq.) in 1.6mL of dry THF were added, the reaction mixture being stirred for 10 minutes more at room temperature. 5-Ethynylbenzo[b]thiophene (431.34 mg; 2.73 mmol; 1 eq.) was then added followed by dry MeOH (218.40 μL , 5.4 mmol). The reaction mixture was stirred at room temperature until no starting material was detected by TLC (4 hours). After this time, the reaction mixture was filtered through a pad of celite and the residue was purified by column chromatography on silica gel (hexane-EtOAc 9:1) obtaining a white solid in 68% yield.

White solid; $R_f=0.51$ (hexane-EtOAc 9:1); $^1\text{H-NMR}$ (CDCl_3 , 300MHz): $\delta= 7.88$ (d, $J=1.5$ Hz, 1H), 7.83 (d, $J=8.3$ Hz, 1H), 7.58-7.46 (m, 2H), 7.44 (d, $J=5.5$ Hz, 1H), 7.33 (dd, $J=5.5, 0.7$ Hz, 1H), 6.23 (d, $J=18.4$ Hz, 1H), 1.33 (s, 12H). $^{13}\text{C-NMR}$ (CDCl_3 , 75 MHz): $\delta= 149.77, 140.37, 140.05, 134.14, 127.09, 124.27, 122.94, 122.84, 122.64, 83.48, 24.96$. MS (EI) m/z 288.15 (M^{+2} , 6.3), 287.15 (M^{+1} , 19.3), 286.10 (M^+ , 100), 285.15 (M^{+1} , 24.7), 228.10 (7.4), 201.10 (21.8), 186.00 (95), 170.00 (74.5), 160.00 (14.9), 134.00 (14.7), 115.05 (13.1), 89.05 (5.2), 57.10 (3.9). IR (neat) ν_{max} 2977.55, 2937.41, 1693.19, 1619.91, 1430.92, 1353.78, 1322.93, 1214.93, 1137.80, 1049.09, 998.95, 971.95, 898.67, 844.67, 798.39, 759.82, 698.11, 659.54cm^{-1} .



(E)-2-(2-(Benzo[b]thiophen-6-yl)vinyl)-4,4,5,5-tetramethyl-1,3,2-dioxaborolane (6)⁵

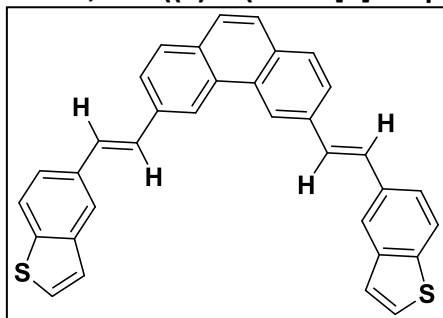
This compound was prepared employing the previous procedure, replacing the terminal alkyne by 6-

ethynylbenzo[b]thiophene.

Yellow oil in 83% yield; $R_f=0.44$ (hexane-EtOAc 9:1); $^1\text{H-NMR}$ (CDCl_3 , 300MHz): $\delta= 7.94$ (d, $J=0.6$ Hz, 1H), 7.77 (d, $J=8.3$ Hz, 1H), 7.55 (dd, $J=8.1, 1.6$ Hz, 1H), 7.51 (d, $J= 18.4$ Hz, 1H), 7.45 (d, $J=5.4$ Hz, 1H), 7.30 (d, $J=5.4$ Hz, 1H), 6.24 (d, $J=18.4$ Hz, 1H), 1.33 (s, 12H). $^{13}\text{C-NMR}$ (CDCl_3 , 75 MHz): $\delta= 149.51, 140.27, 140.21, 134.07, 127.66, 123.87, 123.71, 123.06, 121.80, 83.48, 24.94$. MS (EI) m/z 288.10 (M^{+2} , 6.7), 287.10 (M^{+1} , 19.3), 286.10 (M^+ , 100), 285.15 (M^{+1} , 24.2), 271.10 (12.6), 228.10 (5.9), 201.10 (20.9), 186.00 (82.9), 170.00 (69.3), 161.00 (15.4), 134.00 (12.5),

115.05 (11.1), 89.05 (4.6), 57.10 (3.4). IR (neat) ν_{max} 2977.55, 2927.41, 1689.34, 1619.91, 1457.92, 1346.07, 1265.07, 1207.22, 1141.65, 1041.37, 998.95, 894.81, 844.67, 813.81, 736.67, 694.25 cm^{-1} .

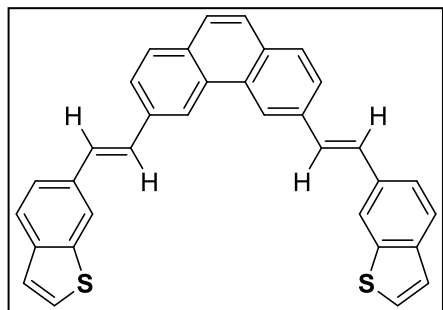
4.3. 3,6-Bis((E)-2-(benzo[b]thiophen-5-yl)vinyl)phenanthrene (8)



This compound was prepared by adapting to our substrates a Suzuki coupling described in the literature⁶. In an over-dried pressure tube PdCl₂ (19.30 mg; 0.11 mmol; 0.20 eq.), PPh₃ (62.50 mg; 0.21 mmol; 0.40 eq.), Cs₂CO₃ (1.03 g; 3.42 mmol; 6 eq.), (E)-2-(2-(benzo[b]thiophen-5-yl)vinyl)-4,4,5,5-tetramethyl-1,3,2-dioxoborolane (524.40 mg; 1.71 mmol; 3 eq.) and 3,6-dibromophenanthrene (176.40 mg; 0.57 mmol; 1 eq.) were added. The tube was sealed with a septum and after three cycles of vacuum/argon, 3.6 mL of THF and 0.4 mL of H₂O were added with a syringe. Then the tube was closed and heated in an oil bath at 85°C for 20 hours. An insoluble solid in suspension was observed in the tube. The insoluble solid, a greenish yellow solid, was filtered and washed with H₂O and CH₂Cl₂ (10 mL each).

Greenish solid in 90% yield; R_f = 0.48 (hexane-EtOAc 9:1); ¹H-NMR (CDCl₃, 400MHz): δ = 8.80 (s, 2H), 8.03 (s, 2H), 7.91 (d, J = 8.4 Hz, 2H), 7.89 (m, 4H), 7.72 (s, 2H), 7.69 (dd, J = 8.4, 1.5 Hz, 2H), 7.53-7.44 (m, 6H), 7.39 (d, J = 5.4 Hz, 2H). MS (EI, DIP) m/z 496.2 (M^+ +2, 14.33), 495.2 (M^+ +1, 32.40), 494.2 (M^+ , 100), 358.2 (11.33), 247.1 (16.42). IR (neat) ν_{max} 3054.69, 1511.92, 1434.78, 1326.79, 1261.22, 1045.23, 960.37, 887.09, 840.81, 806.09, 752.10, 694.24.

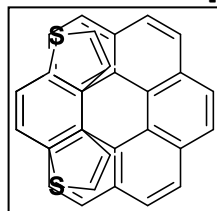
3,6-Bis((E)-2-(benzo[b]thiophen-6-yl)vinyl)phenanthrene (9)



This compound was prepared following the previous procedure, but as starting reagents (E)-2-(2-(benzo[b]thiophen-6-yl)vinyl)-4,4,5,5-tetramethyl-1,3,2-dioxoborolane and 3,6-dibromophenanthrene were used.

Greenish solid in 95% yield; R_f = 0.44 (hexane-EtOAc 9:1); ¹H-NMR (CDCl₃, 300MHz): δ = 8.81 (s, 2H), 8.10 (s, 2H), 7.89 (s, 4H), 7.86 (d, J = 8.3 Hz, 2H), 7.72 (s, 2H), 7.69 (dd, J = 8.3, 1.5 Hz, 2H), 7.50-7.46 (m, 6H), 7.36 (d, J = 4.7 Hz, 2H). MS (EI, DIP) m/z 496.2 (M^+ +2, 16.33), 495.2 (M^+ +1, 38.06), 494.2 (M^+ , 100), 358.2 (11.64), 247.1 (16.07). IR (neat) ν_{max} 3062.41, 3023.84, 1600.63, 1392.35, 1083.80, 1041.37, 956.52, 879.38, 836.95, 752.10, 694.25.

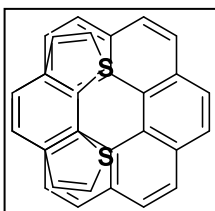
4.4. Exo-dithia[9]helicene (1)



The synthesis of this compound has been carried out by three photochemical methods (A, B and C) in line what was explained above (photochemistry). Method A) in three oven-dried Schlenk tubes were loaded with 3,6-bis((E)-2-(benzo[b]thiophen-5-yl)vinyl)phenanthrene (49.42 mg; 0.1 mmol; 1 eq.), KI (33.2 mg; 0.2 mmol; 2 eq.) and 200 mL of benzene each. The tubes were provided with vertical condensers connected in line to a chiller. The recirculation chiller was turned on and the mixture was irradiated with a 400 W high-pressure Hg lamp for 3-4 hours under continuous reflux. Method B) in a different procedure under inert atmosphere a suspension of 3,6-bis((E)-2-(benzo[b]thiophen-5-

yl)vinyl)phenanthrene (24.71 mg; 0.05 mmol; 1 eq.), iodine (38.07 mg; 0.15 mmol; 3 eq.), 1,2-epoxybutane (360.5 mg; 5 mmol; 100 eq.) and 100mL of benzene were placed in an oven-dried Schlenk tubes. As in the former method, the recirculation chiller was turned on and the mixture was irradiated with 400 W high-pressure Hg lamp for 3-4 hours in refluxing benzene under Ar. Method C) LED technology. In here we used the same amount of reagents a in B to compare reaction time and yields. The Schlenk tubes were safely irradiated with our LED setup overnight (12 h) at room temperature. In all cases, (A, B and C) the advance of the reaction was followed by TLC. After the reaction was completed, it was washed with aqueous NaHSO₃, dried over magnesium sulfate, filtered and the solvent evaporated under reduced pressure (15 Torr). The residue was purified by column chromatography on silica gel (hexane- CH₂Cl₂ 8:2) to obtain a greenish yellow solid. The isolated yields are: Methos A) 3-4 h, 52%. Methos B) 3-4 h, 49%. Method C) 12 h, 60%.

Greenish yellow crystals; approximated melting point 365.3°C (DSC, with decomposition); *R*_f= 0.39 (hexane-CH₂Cl₂/8:2); ¹H-NMR (Methylene chloride-d₂, 400MHz): δ= 8.09 (s, 2H), 7.98 (d, *J*=8.1 Hz, 2H), 7.67 (d, *J*=8.2 Hz, 2H), 7.44 (dd, *J*=8.5 0.8 Hz, 2H), 7.27 (d, *J*=8.4 Hz, 2H), 7.23 (d, *J*=8.4 Hz, 2H), 7.18 (d, *J*=8.5 Hz, 2H), 6.50 (dd, *J*=5.5 0.4 Hz, 2H), 6.00 (dd, *J*=5.5 0.8 Hz, 2H). ¹³C-NMR (Methylene Chloride-d₂, 101 MHz): δ= 138.23, 134.04, 132.82, 131.86, 129.93, 127.81, 127.14, 127.08, 127.02, 126.93, 126.17, 125.91, 124.96, 124.70, 122.98, 122.69, 120.56. MS (EI, DIP) *m/z* 492.1 (M⁺+2, 14.80), 491.1 (M⁺+1, 37.81), 490.1 (M⁺, 100), 456.1 (12.38), 278.1 (13.31), 245.0 (10.78), 228.1 (17.32). HRMS (ESI): M⁺ found 490.0834 [C₃₄H₁₈S₂]⁺, requires 490.0850. IR (neat) *v*_{max} 3035.41, 1465.63, 1346.07, 1315.21, 1191.79, 1157.08, 1130.08, 1091.51, 1014.37, 948.81, 883.24, 836.95, 744.39, 694.25 cm⁻¹.



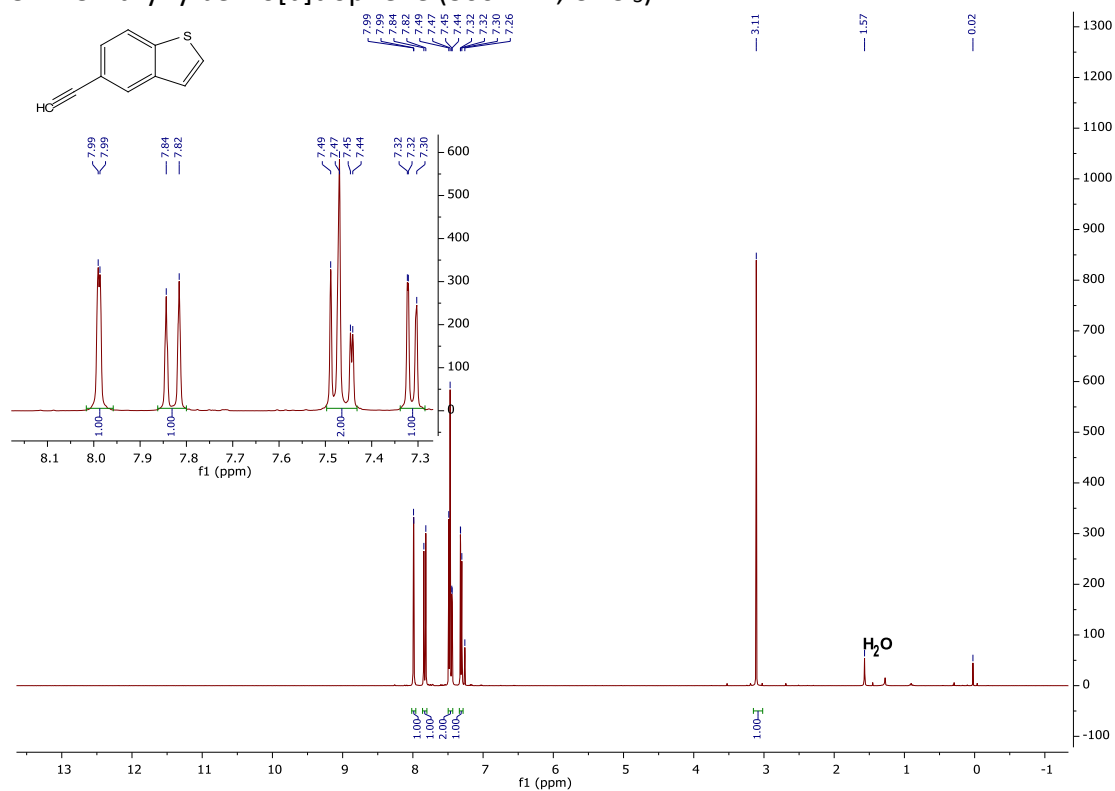
Endo-dithia[9]helicene (2)

In this case a suspension of 3,6-bis((E)-2-(benzo[*b*]tiophen-6-yl)vinyl)phenanthrene, iodine and 1,2-epoxybutane in benzene under Ar, was irradiated following the same methodology described above for the *exo* isomer. The isolated yields are: Method B) 38%. Method C) 48%. The reaction affords only a mixture of unidentifiable products in the presence of air.

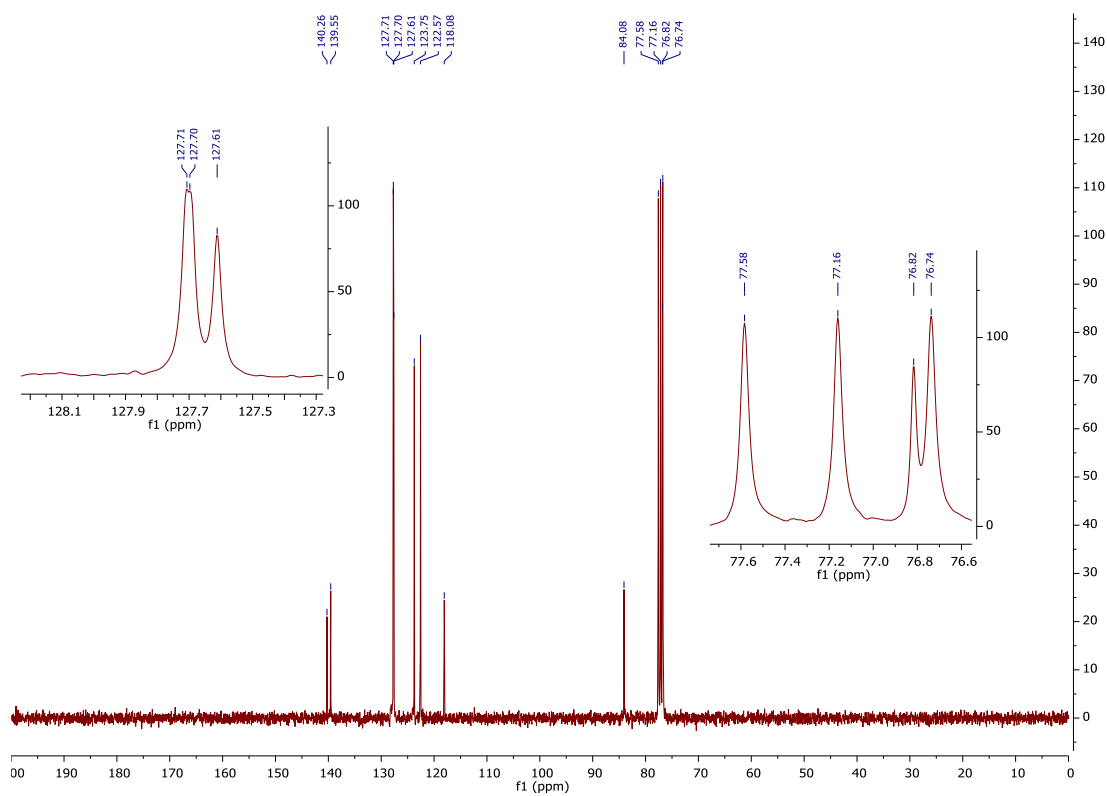
Greenish yellow crystals; approximated 332.3°C melting point (DSC, with decomposition); *R*_f= 0.40 (Hexane-CH₂Cl₂/8:2); ¹H-NMR (CDCl₃, 300MHz): δ= 8.16 (s, 2H), 8.01 (d, *J*=8.1 Hz, 2H), 7.70 (d, *J*=8.2 Hz, 2H), 7.40 (d, *J*=8.4 Hz, 2H), 7.26 (d, *J*=8.4 Hz, 2H), 7.22-7.18 (m, 4H), 6.88 (d, *J*=5.4 Hz, 2H), 6.72 (d, *J*=5.4 Hz, 2H). ¹³C-NMR (CDCl₃, 101 MHz): δ= 137.80, 134.96, 132.63, 132.38, 129.17, 127.42, 127.31, 127.07, 126.59, 126.06, 125.43, 124.74, 124.58, 124.12, 123.69, 122.12, 121.23. MS (EI, DIP) *m/z* 492.2 (M⁺+2, 15.66), 491.2 (M⁺+1, 39.86), 490.2 (M⁺, 100), 443.2 (25.25), 228.1 (15.25). HRMS (ESI): M⁺ found 490.0840 [C₃₄H₁₈S₂]⁺, requires 490.0850. IR (neat) *v*_{max} 3039.26, 1488.78, 1353.78, 1292.07, 1249.65, 1133.94, 1079.94, 948.81, 894.81, 833.10, 736.67, 701.96 cm⁻¹.

5. ^1H NMR and ^{13}C NMR spectra of compounds

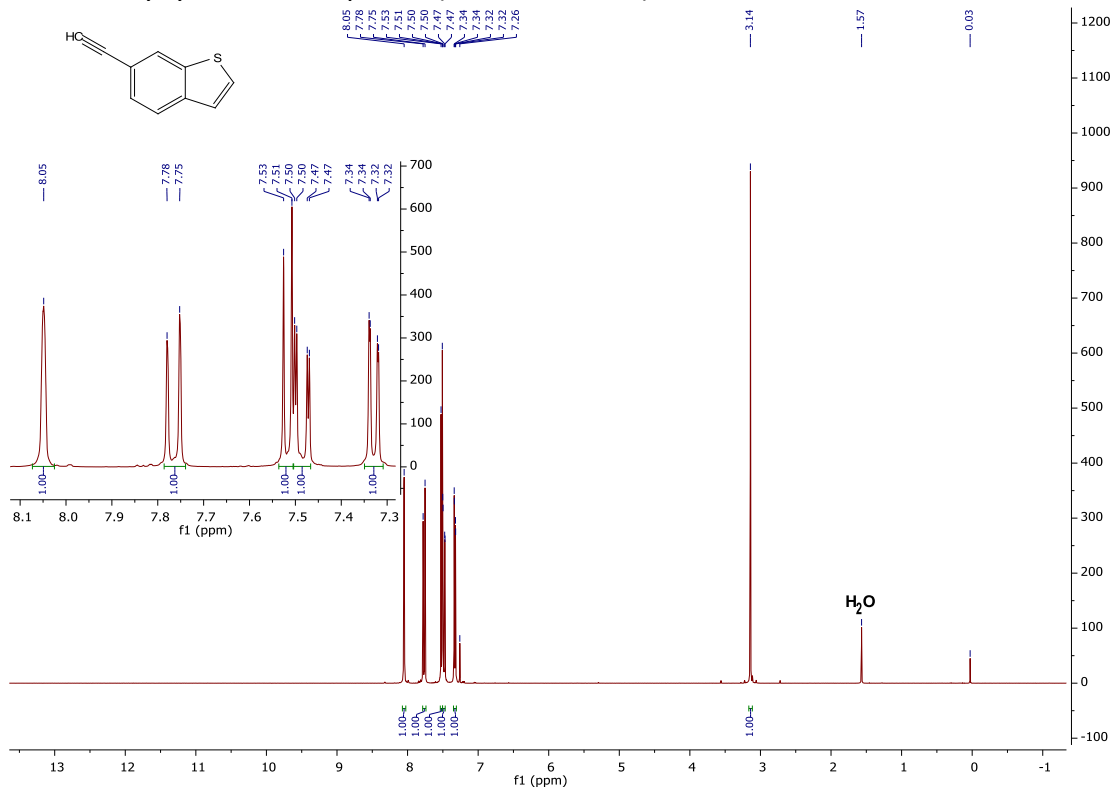
5.1. 5-Ethynylbenzo[*b*]thiophene (300MHz, CDCl_3)



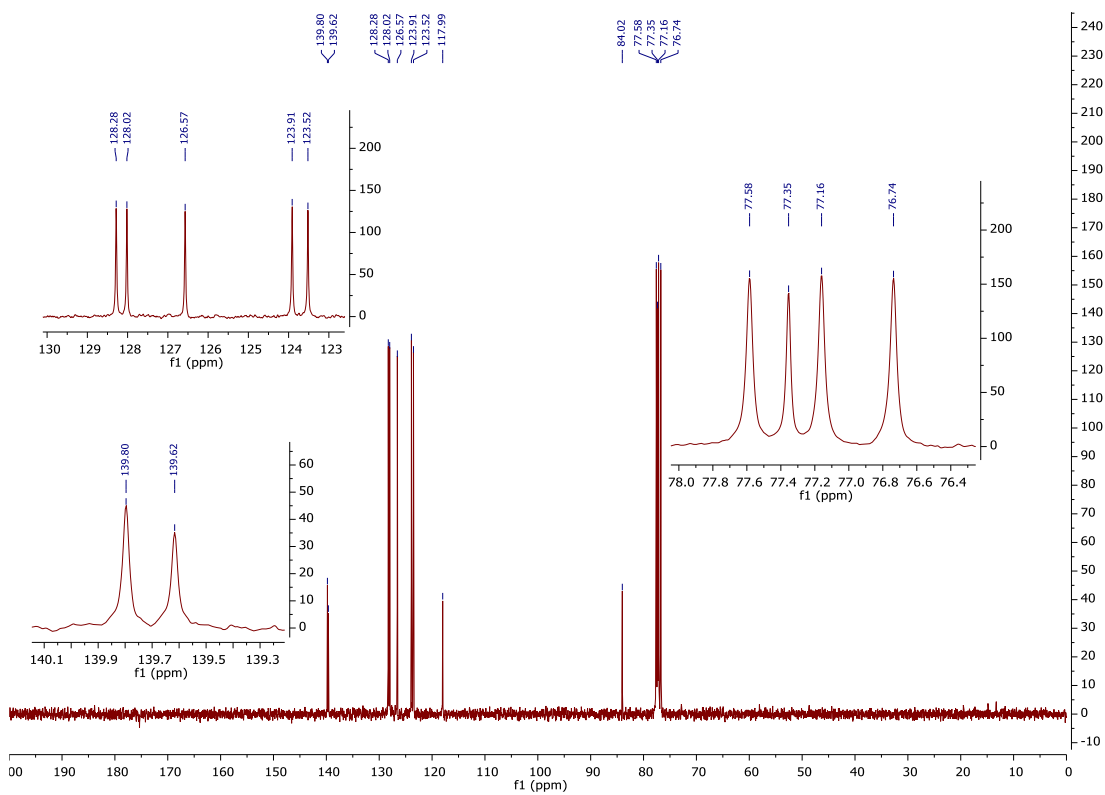
5-Ethynylbenzo[*b*]thiophene (75MHz, CDCl_3)



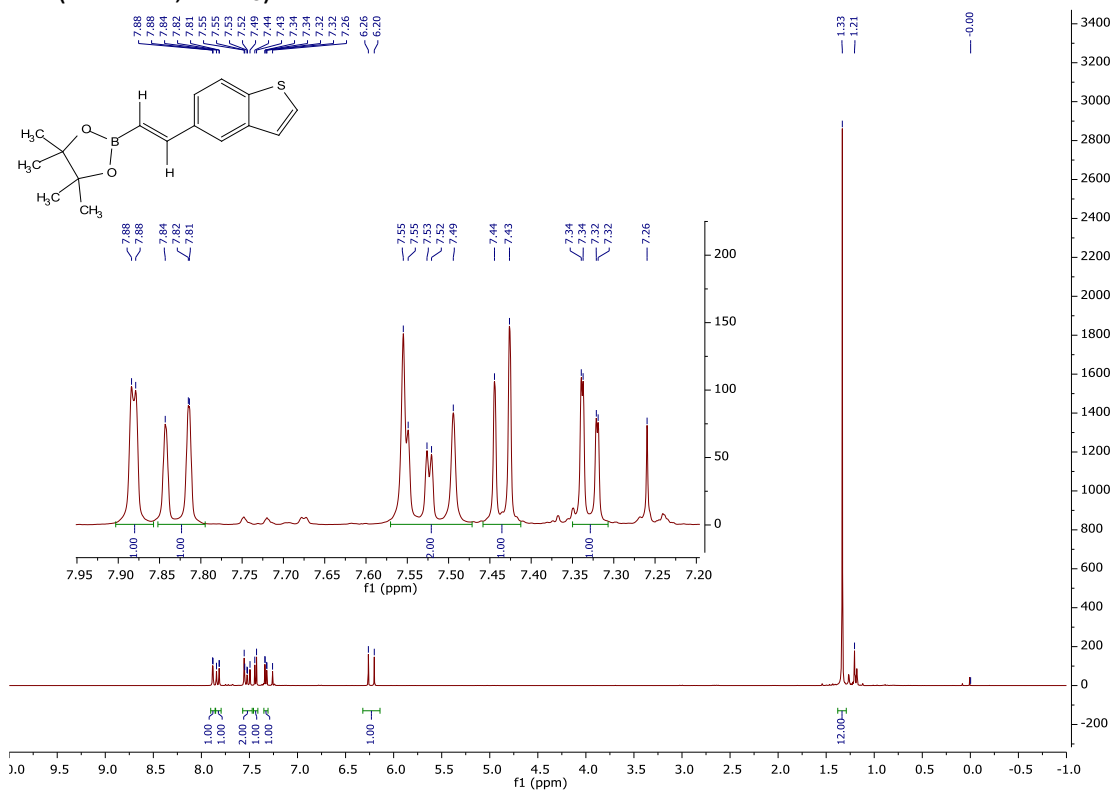
5.2. 6-Ethynylbenzo[*b*]tiophene (300MHz, CDCl₃)



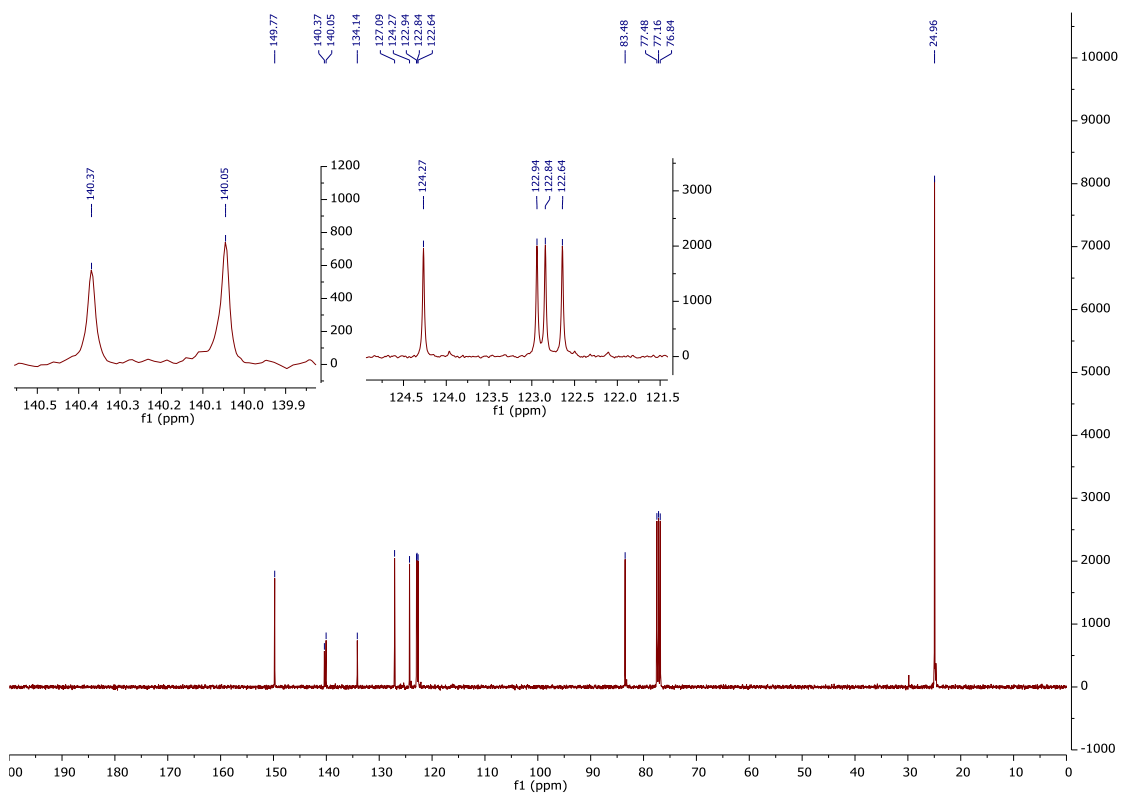
6-Ethynylbenzo[*b*]tiophene (75MHz, CDCl₃)



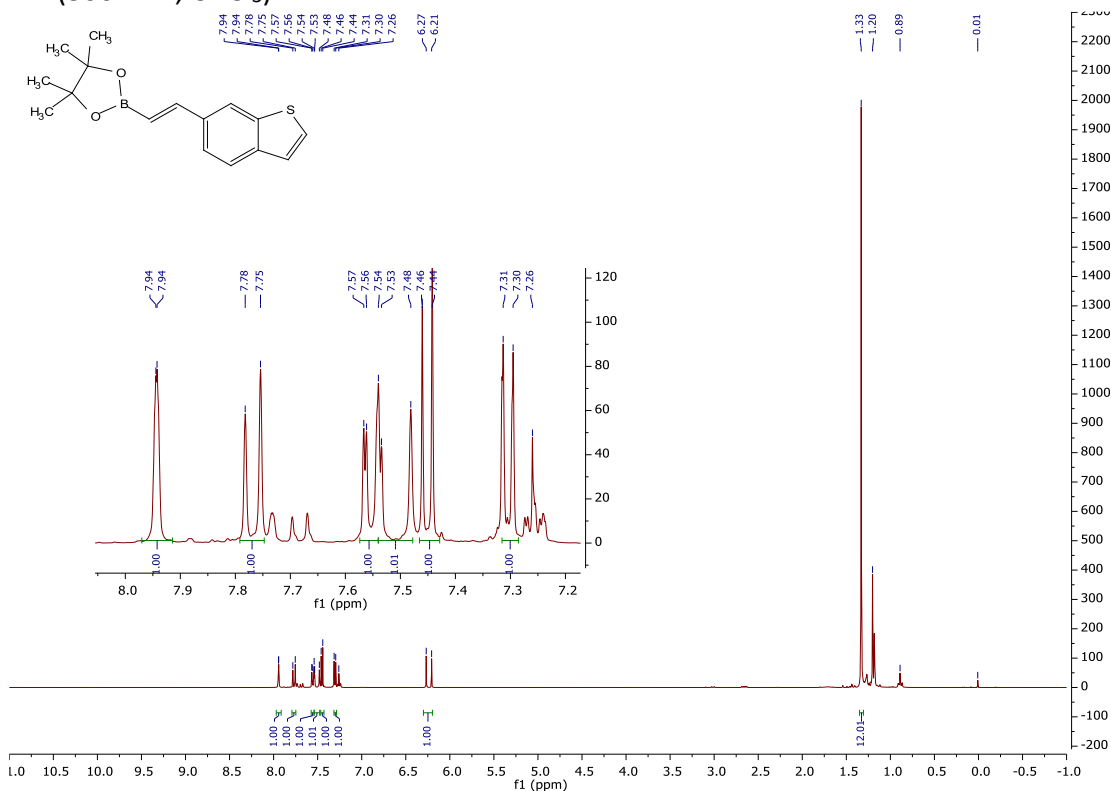
5.3. (*E*)-2-(2-(Benzo[*b*]thiophene-5-yl)vinyl)-4,4,5,5-tetramethyl-1,3,2-dioxaborolane
(300MHz, CDCl₃)



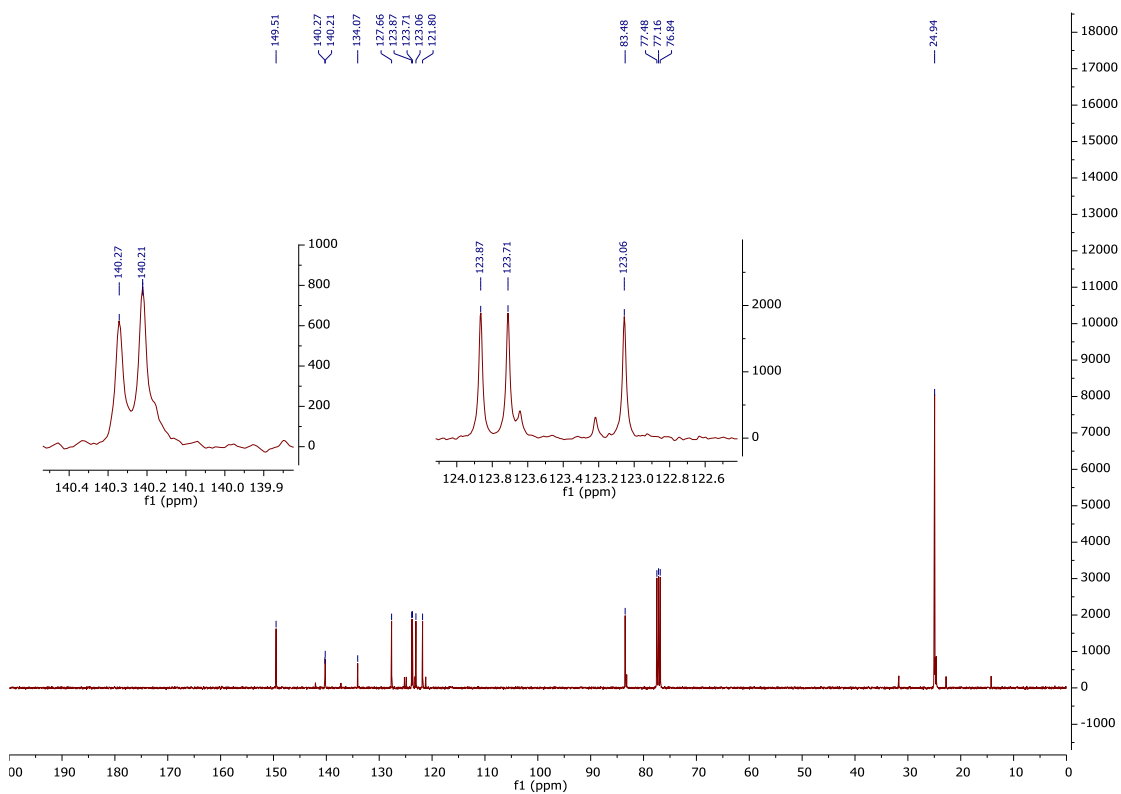
(*E*)-2-(2-(Benzo[*b*]thiophene-5-yl)vinyl)-4,4,5,5-tetramethyl-1,3,2-dioxaborolane
(75MHz, CDCl₃)



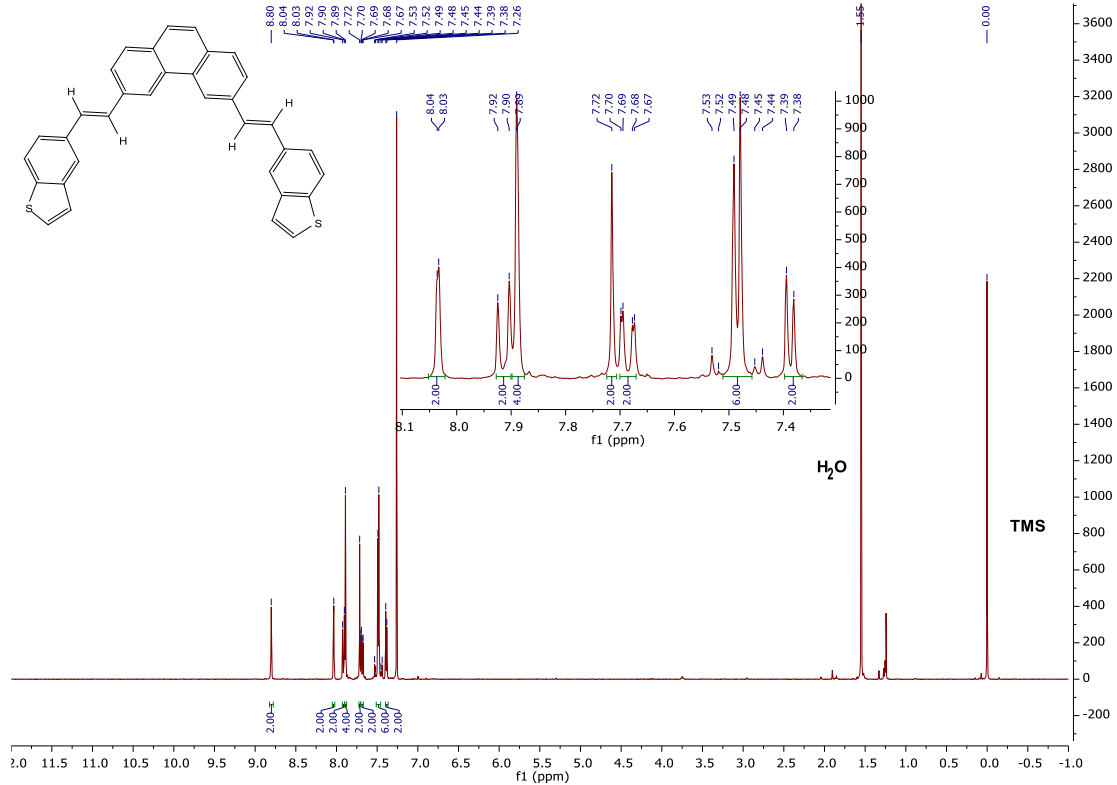
5.4. (*E*)-2-(2-(Benzo[*b*]thiophene-6-yl)vinyl)-4,4,5,5-tetramethyl-1,3,2-dioxaborolane
(300MHz, CDCl₃)



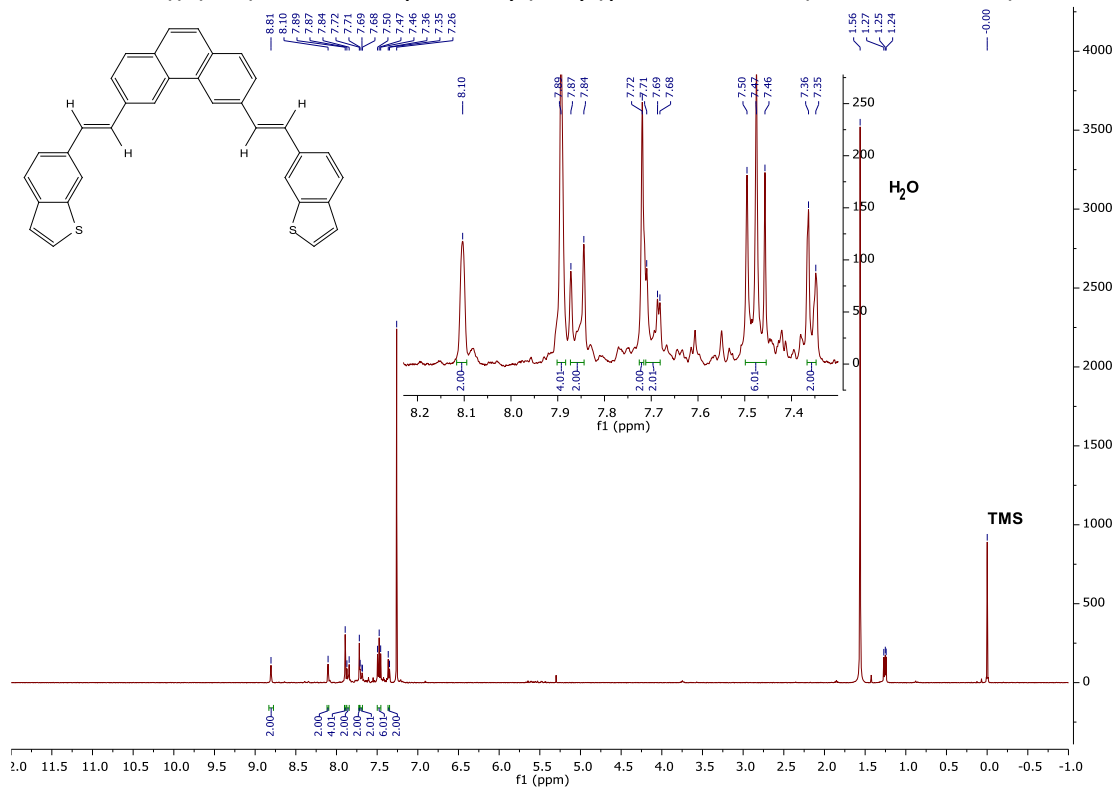
(*E*)-2-(2-(Benzo[*b*]thiophene-6-yl)vinyl)-4,4,5,5-tetramethyl-1,3,2-dioxaborolane
(75MHz, CDCl₃)



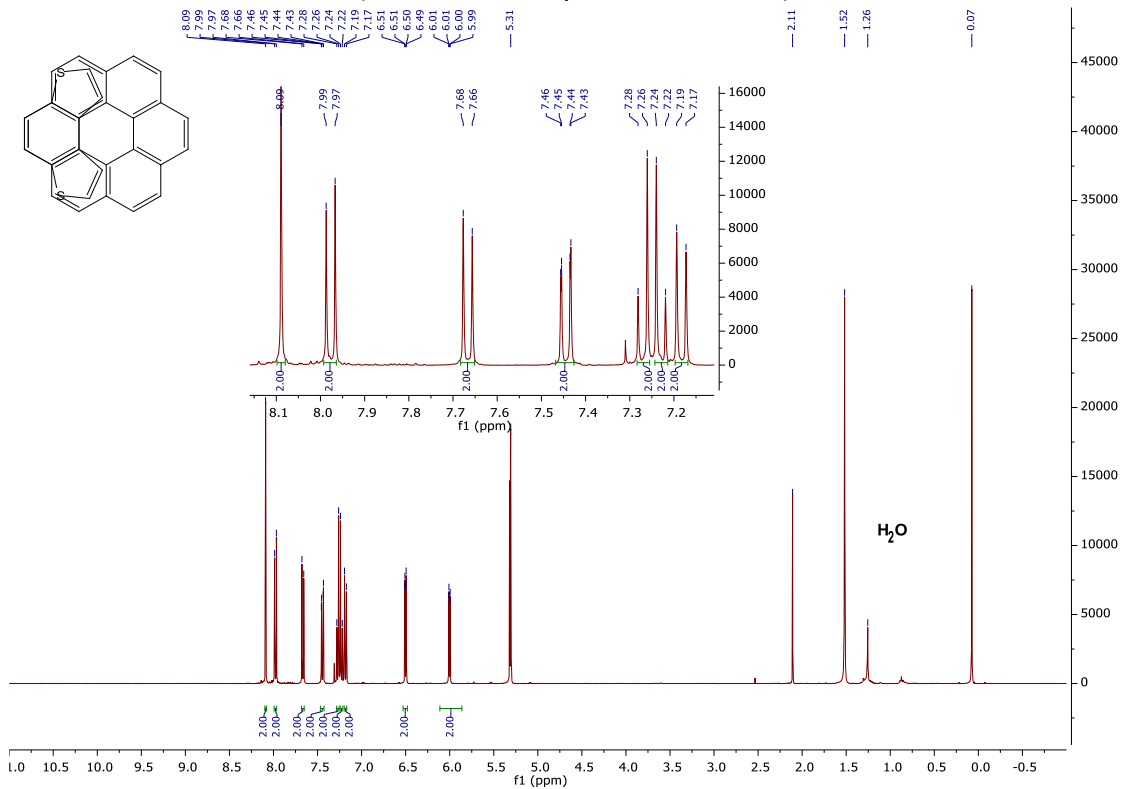
5.5. 3,6-Bis((E)-2-(benzo[b]tiophen-5-yl)vinyl)phenanthrene (400MHz, CDCl₃)



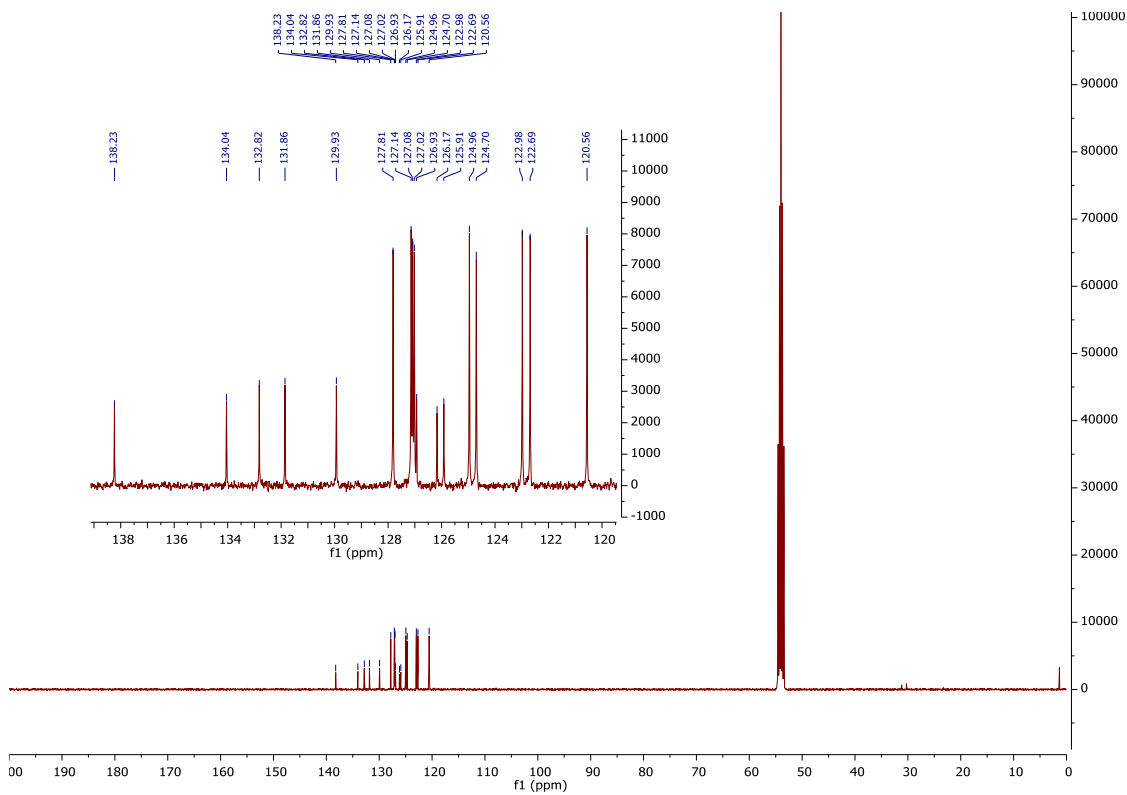
5.6. 3,6-Bis((E)-2-(benzo[b]tiophen-6-yl)vinyl)phenanthrene (300MHz, CDCl₃)



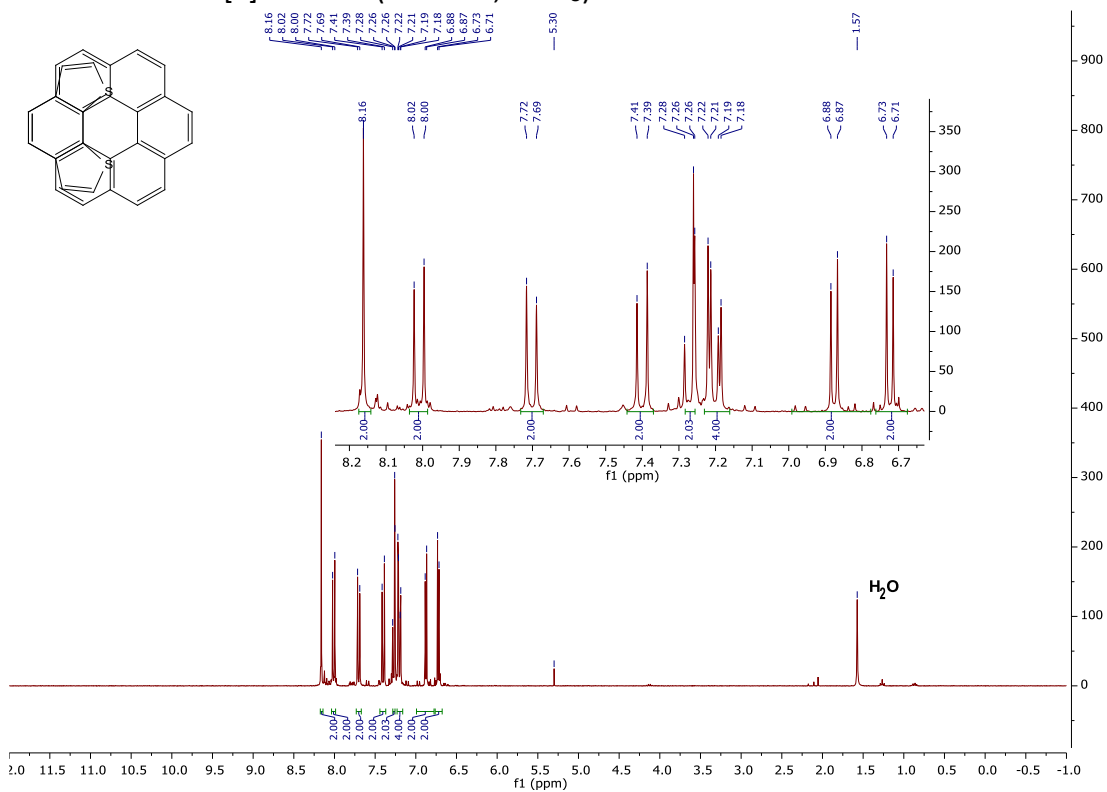
5.7. Exo-dithia[9]helicene (400MHz, Methylene chloride-d₂)



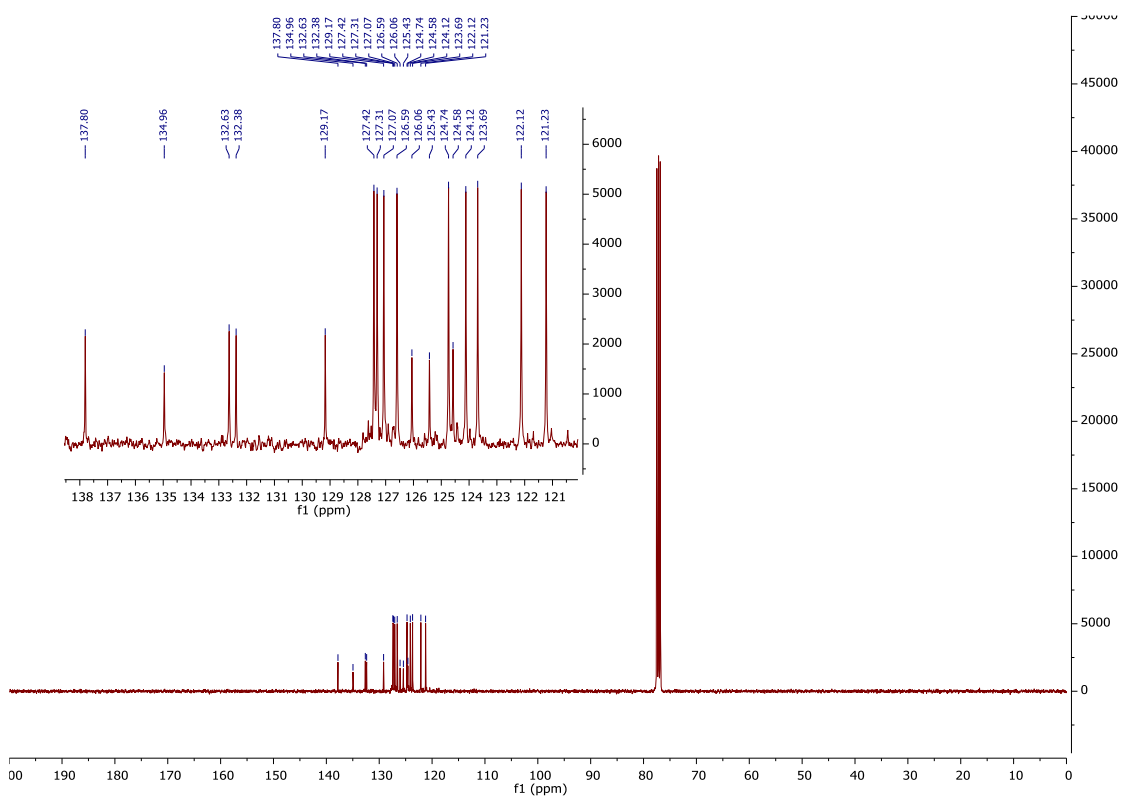
Exo-dithia[9]helicene (101MHz, Methylene chloride-d₂)



5.8. *Endo*-dithia[9]helicene (300MHz, CDCl₃)



Endo-dithia[9]helicene (101MHz, CDCl₃)



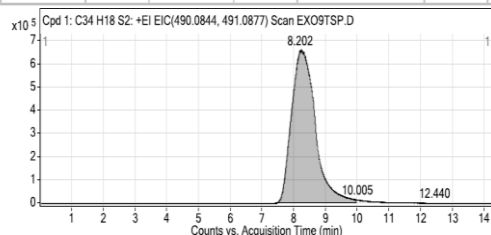
6. HMRS (ESI)

Exo-dithia[9]dithiahelicene

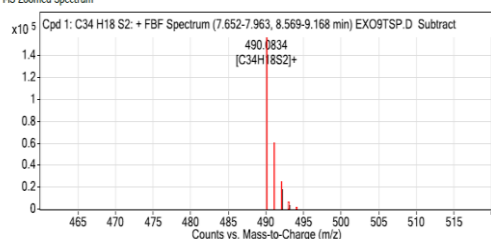
Compound Table

Tgt Formula	Tgt Mass	Obs. Mass	Tgt Score	Mass Error (ppm)	Obs. m/z	Ret.T	Find Comp. Algorithm
C34 H18 S2	490.085	490.084	94.03	-2.12	490.0834	8.202	Find By Formula

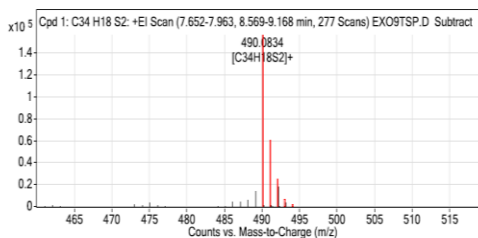
Tgt Formula	Tgt Mass	Obs. Mass	Tgt Score	Mass error (ppm)	Obs. m/z	Find Cps Algorith
C34 H18 S2	490.085	490.084	94.03	-2.12	490.0834	Find By Formula



MS Zoomed Spectrum



Target Compound Screening Report



MS Spectrum Peak List

Obs. m/z	Charge	Abund	Formula	Ion/Isotope	Tgt Mass Error (ppm)
490.0834	1	156467.05	C34H18S2	M+	
491.0864	1	53191.29	C34H18S2	M+	
492.0895	1	18245.49	C34H18S2	M+	
493.0851	1	4272.97	C34H18S2	M+	
494.0849	1	905.35	C34H18S2	M+	
495.0894	1	174.7	C34H18S2	M+	
490.0834	1	156467.05	C34H18S2	M+	2.17
491.0864	1	53191.29	C34H18S2	M+	2.45
492.0895	1	18245.49	C34H18S2	M+	1.05
493.0851	1	4272.97	C34H18S2	M+	1.21
494.0849	1	905.35	C34H18S2	M+	0.48
495.0894	1	174.7	C34H18S2	M+	2.32

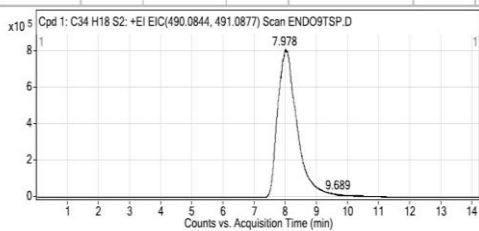
-- End Of Report --

Endo-dithia[9]helicene

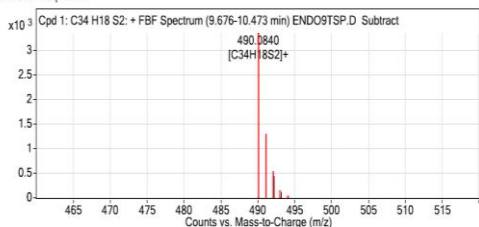
Compound Table

Tgt Formula	Tgt Mass	Obs. Mass	Tgt Score	Mass Error (ppm)	Obs. m/z	Ret.T	Find Comp. Algorithm
C34 H18 S2	490.085	490.0846	98.21	-0.77	490.084	9.689	Find By Formula

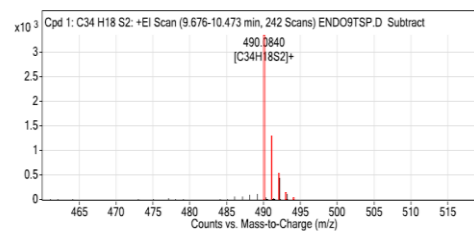
Tgt Formula	Tgt Mass	Obs. Mass	Tgt Score	Mass error (ppm)	Obs. m/z	Find Cps Algorith
C34 H18 S2	490.085	490.0846	98.21	-0.77	490.084	Find By Formula



MS Zoomed Spectrum



Target Compound Screening Report



MS Spectrum Peak List

Obs. m/z	Charge	Abund	Formula	Ion/Isotope	Tgt Mass Error (ppm)
490.084	1	3339.65	C34H18S2	M+	
491.0872	1	1190.11	C34H18S2	M+	
492.085	1	446.68	C34H18S2	M+	
493.0857	1	124.15	C34H18S2	M+	
494.0846	1	32.72	C34H18S2	M+	
490.084	1	3339.65	C34H18S2	M+	0.84
491.0872	1	1190.11	C34H18S2	M+	0.92
492.085	1	446.68	C34H18S2	M+	0
493.0857	1	124.15	C34H18S2	M+	0.06
494.0846	1	32.72	C34H18S2	M+	1.09

-- End Of Report --

7. X-ray diffraction (XRD) analysis

The crystals of *exo*-dithia[9]helicene-1 and *endo*-dithia[9]helicene-2 were analyzed using a Bruker CCD-Apex single crystal X-Ray diffraction kit equipped with an X-ray tube with Mo anode and KRYOFLEX low temperature equipment.

Exo-dithia[9]helicene-1

Bond precision: C-C = 0.0176 Å

Wavelength=0.71073

Cell: a=33.075(4) b=9.8984(11) c=28.178(3)

alpha=90 beta=94.890(2) gamma=90

Temperature: 298 K

	Calculated	Reported
Volume	9191.6 (18)	9191.7 (17)
Space group	C 2/c	C 2/c
Hall group	-C 2yc	
Moiety formula	C ₃₄ H ₁₈ S ₂	C ₃₄ H ₁₈ S ₂
Sum formula	C ₃₄ H ₁₈ S ₂	C ₃₄ H ₁₈ S ₂
Mr	490.60	490.60
Dx, g cm ⁻³	1.418	1.418
Z	16	16
Mu (mm ⁻¹)	0.255	0.255
F 0 0 0	4064.0	4064.0
F 0 0 0'	4069.33	
h, k, l max	39, 11, 33	39, 11, 33
Nref	8147	8132
Tmin, Tmax	0.982, 0.995	0.932, 0.995
Tmin'	0.912	

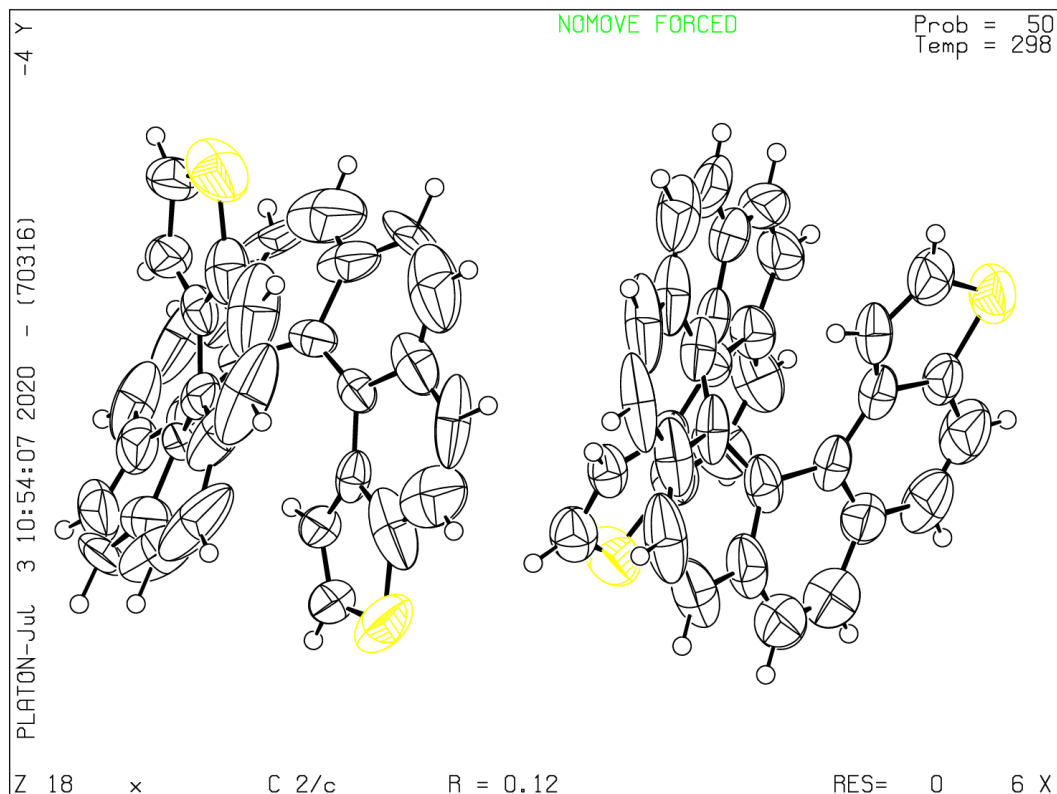
Correction method= # Reported T Limits: Tmin=0.932 Tmax=0.995

AbsCorr = MULTI-SCAN

Data completeness= 0.998 Theta(max)= 25.050

R(reflections)= 0.1173(3653) wR2(reflections)= 0.3000(8132)

S = 1.021 Npar= 649



Comments to the checkCIF/Platon Exo-dithia[9]helicene-1: deposition number 2184340.
Associated files: x_finalfile001.cif and a380.fcf

a380

Level A

PLAT234 Large Hirshfeld Difference C5 --C6. 0.41 Å.

Response: The most probable cause in here is dynamic disorder along with a limited quality of the crystal. The structure was determined at room temperature, as a low temperature setup was not operative in our facilities. Analysis done considering higher symmetry groups or potential twinning did not afford better results, as neither did several attempts to recrystallize the compound under different conditions. Substitutional disorder or misassignment of atom positions are not the causes for this, nor has the structure been over-refined.

Level B. Response: The same arguments stated above apply in here.

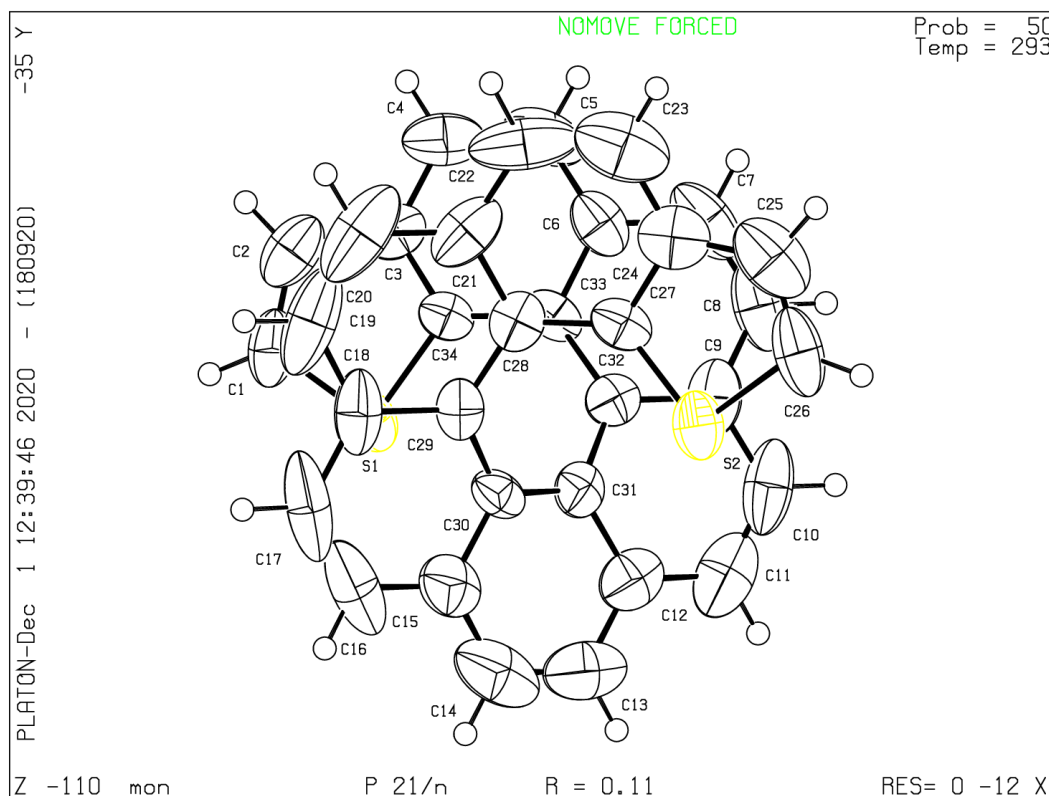
Endo-dithia[9]helicene-2

Bond precision: C-C = 0.0140 Å
Wavelength=0.71073
Cell: a=9.712(2) b=9.709(3) c=25.072(6)
alpha=90 beta=94.401(7) gamma=90
Temperature: 293 K

	Calculated	Reported
Volume	2357.2 (10)	2357.2 (10)

Space group	P 21/n	P 21/n
Hall group	-P 2yn	
Moiety formula	C ₃₄ H ₁₈ S ₂	C ₃₄ H ₁₈ S ₂
Sum formula	C ₃₄ H ₁₈ S ₂	C ₃₄ H ₁₈ S ₂
Mr	490.60	490.60
Dx, g cm ⁻³	1.382	1.382
Z	4	4
Mu (mm ⁻¹)	0.249	0.249
F 0 0 0	1016.0	1016.0
F 0 0 0'	1017.33	
h, k, l max	11, 11, 29	11, 11, 29
Nref	4203	4193
Tmin, Tmax	0.905, 0.995	0.526, 0.995
Tmin'	0.905	

Correction method= # Reported T Limits: Tmin=0.526 Tmax=0.995
AbsCorr = MULTI-SCAN
Data completeness= 0.998 Theta(max)= 25.110
R(reflections)= 0.1078(1054) wR2(reflections)= 0.1439(4193)
S = 0.686 Npar= 325



Comments to the checkCIF/Platon Endo-dithia[9]helicene-2: deposition number 2184341.
Associated files: mon_final003.cif and a387.fcf
a387

RINTA01 The value of Rint is greater than 0.25

Response: The overall quality of the data may be somewhat low because the crystal diffracts only weakly in one of its dimensions. Unfortunately, attempts to obtain better quality crystals

by recrystallizing the compound under different conditions (T/solvent) did not afford better quality data. The structure was determined at room temperature, as a low temperature setup was not operative in our facilities.

PLAT020 The Value of Rint is Greater Than 0.12 0.446 Report

Response: Similar arguments to those described before apply in here.

PLAT026 Ratio Observed / Unique Reflections (too) Low .. 25% Check

Response: Again, a poor diffraction in one of the directions of the crystal may be responsible for this issue. Unfortunately, it could not be solved using different crystals obtained under different conditions of recrystallization, which afforded similar data.

Level B. Response: The same arguments stated above apply in here.

8. List of possible isomeric structures in the synthesis of *exo-1* and *endo-2*

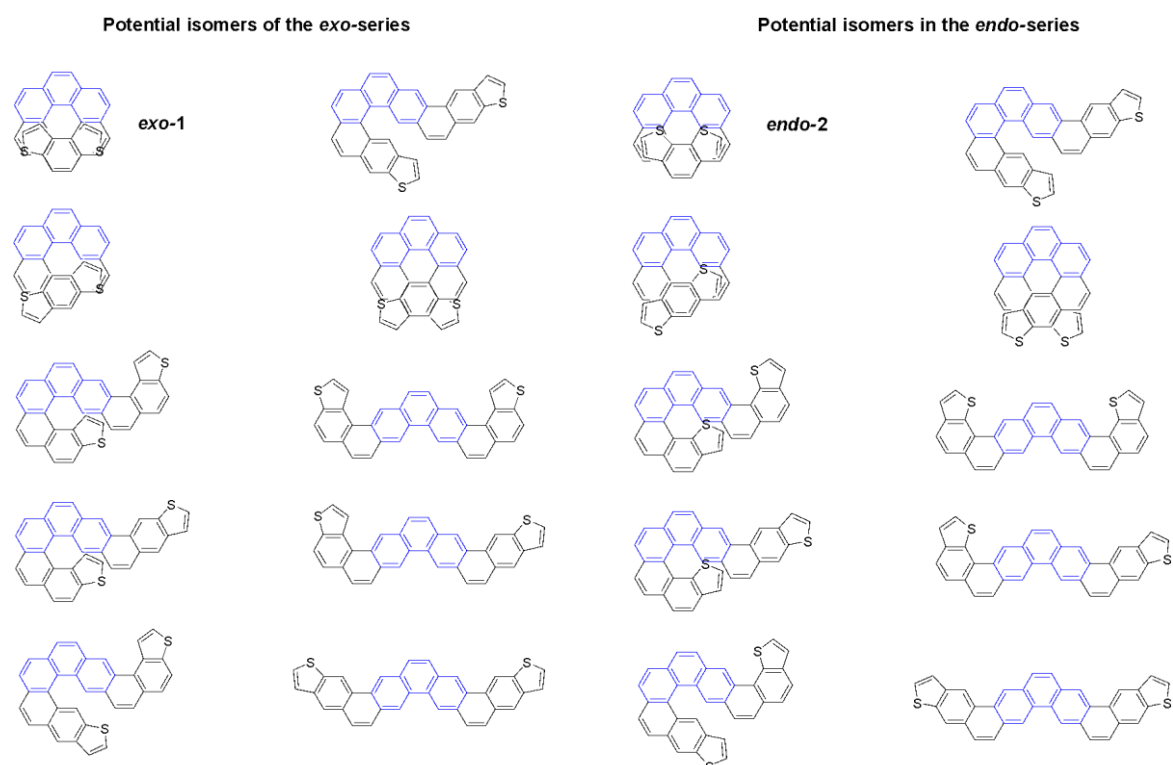


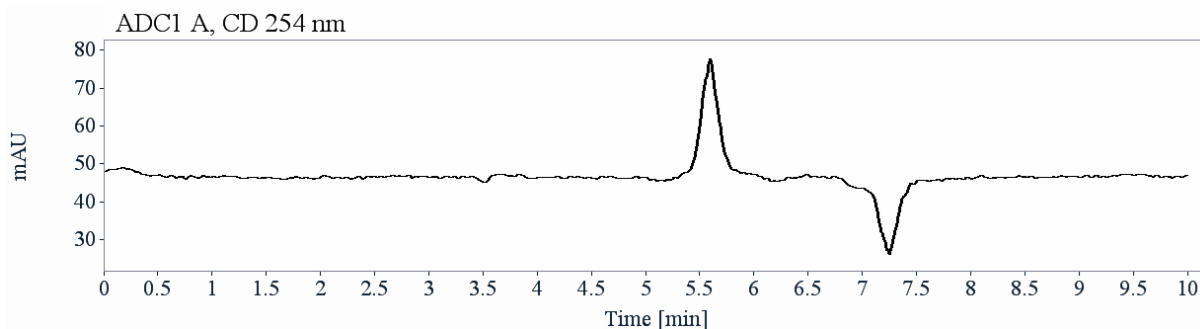
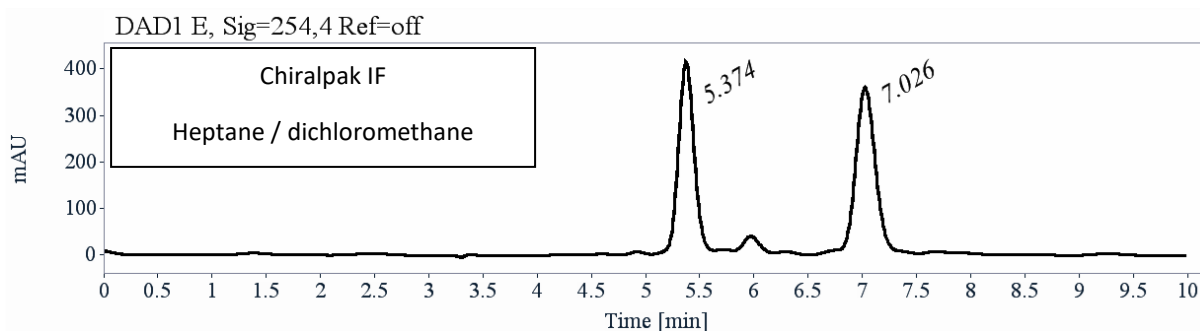
Figure S1. The 10 possible isomers of the *exo* and *endo* series

9. HPLC separations

Analytical chiral HPLC separation for compound 1

- The sample is dissolved in dichloromethane, injected on the chiral column, and detected with a UV detector at 254 nm and a circular dichroism detector at 254 nm. The flow-rate is 1 mL/min.

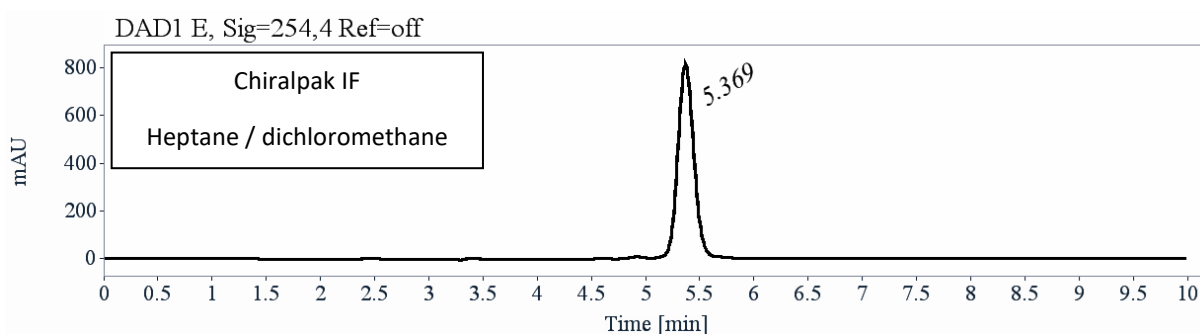
Column	Mobile Phase	t1	k1	t2	k2	α	Rs
Chiralpak IF	Heptane / dichloromethane (70/30)	5.37 (+)	0.82	7.03 (-)	1.38	1.68	5.61



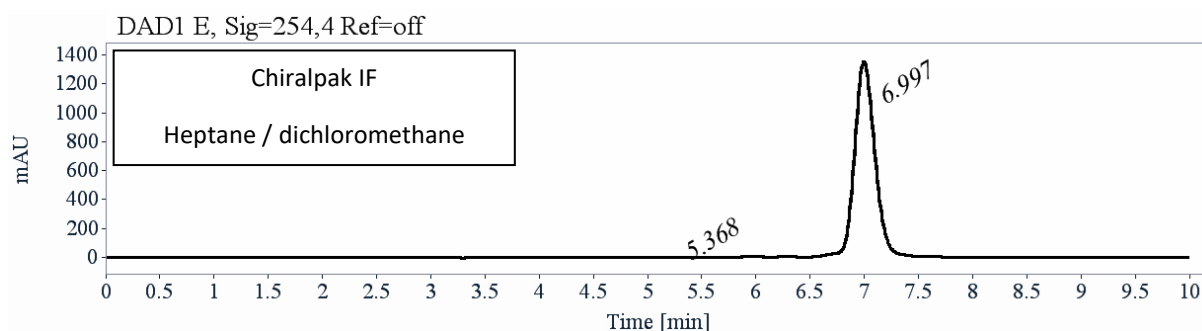
RT [min]	Area	Area%	Capacity Factor	Enantioselectivity	Resolution (USP)
5.37	4079	48.54	0.82		
7.03	4324	51.46	1.38	1.68	5.61
Sum	8402	100.00			

Preparative separation for compound 1:

- Sample preparation: About 40 mg of compound **1** were dissolved in 11 mL of dichloromethane.
- Chromatographic conditions: Chiralpak IF (250 x 4.6 mm), hexane / dichloromethane (70/30) as mobile phase, flow-rate = 1 mL/min, UV detection at 254 nm.
- Injections (stacked): 74 times 150 μ L, every 8.4 minutes.
- First fraction: 12 mg of the first eluted with ee > 99.5 %



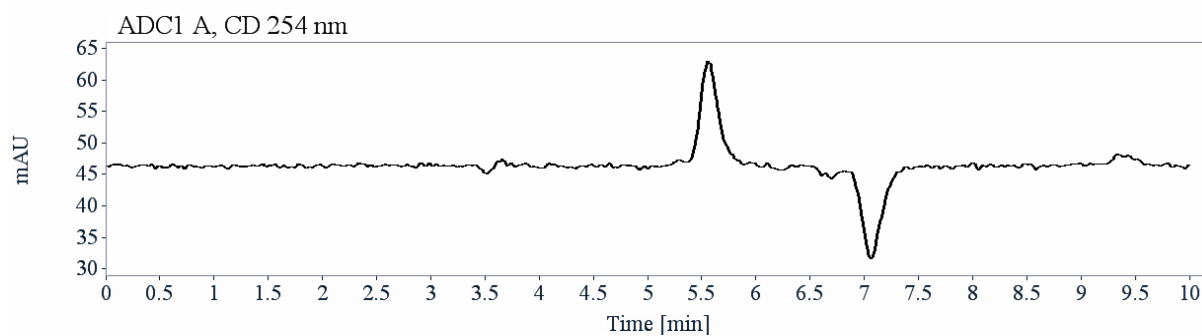
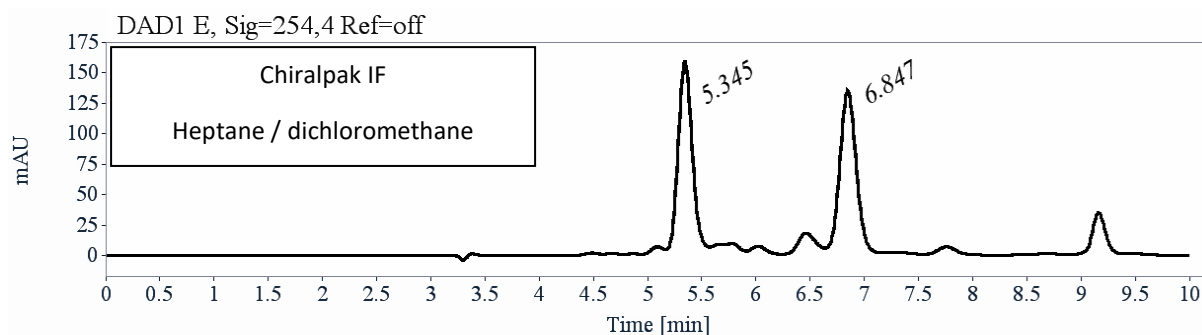
- Second fraction: 14 mg of the second eluted with ee > 99.5 %



Analytical chiral HPLC separation for compound 2

- The sample is dissolved in dichloromethane, injected on the chiral column, and detected with a UV detector at 254 nm and a circular dichroism detector at 254nm. The flow-rate is 1 mL/min.

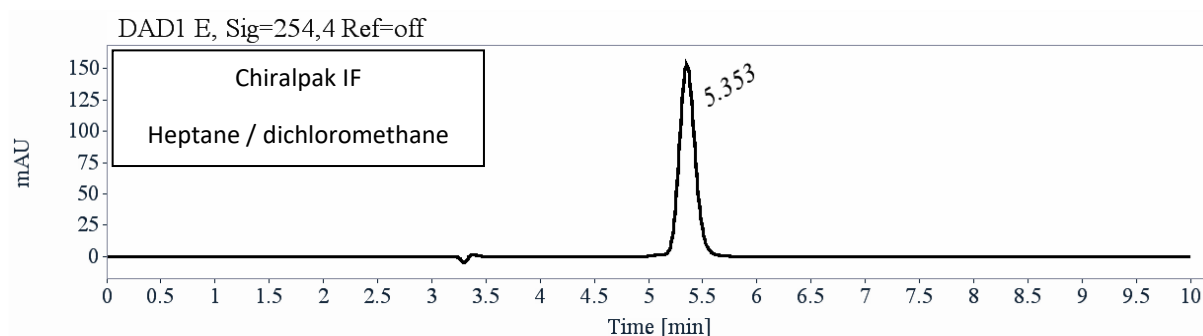
Column	Mobile Phase	t1	k1	t2	k2	α	Rs
Chiralpak IF	Heptane / dichloromethane (70/30)	5.34 (+)	0.81	6.85 (-)	1.32	1.63	5.95



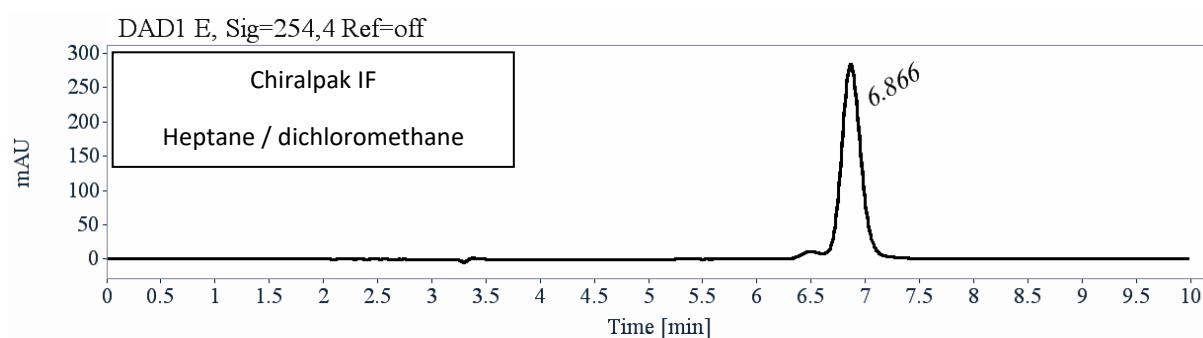
RT [min]	Area	Area%	Capacity Factor	Enantioselectivity	Resolution (USP)
5.34	1344	50.17	0.81		
6.85	1335	49.83	1.32	1.63	5.95
Sum	2678	100.00			

Preparative separation for compound 2:

- Sample preparation: About 16 mg of compound **2** were dissolved in 4 mL of a mixture of dichloromethane and hexane (50/50).
- Chromatographic conditions: Chiralpak IF (250 x 4.6 mm), hexane / dichloromethane (70/30) as mobile phase, flow-rate = 1 mL/min, UV detection at 254 nm.
- Injections (stacked): 20 times 200 μ L, every 8.4 minutes.
- First fraction: 2.5 mg of the first eluted with ee > 99.5 %



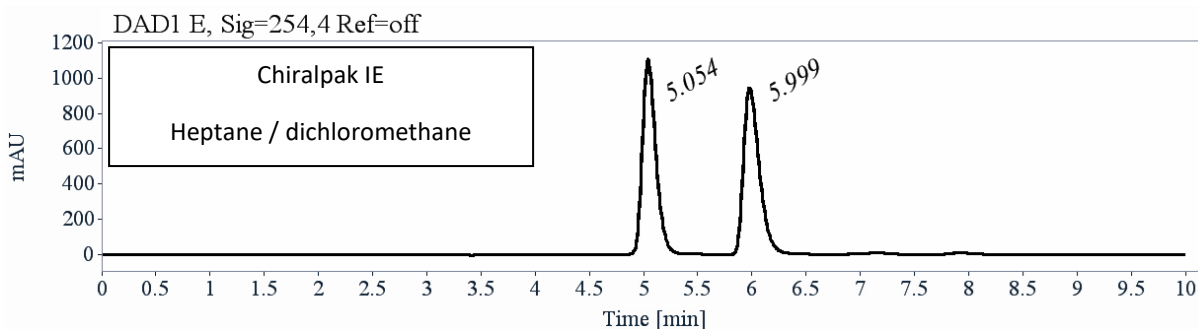
- Second fraction: 3.3 mg of the second eluted with ee > 99.5 %



Analytical chiral HPLC separation for compound 10

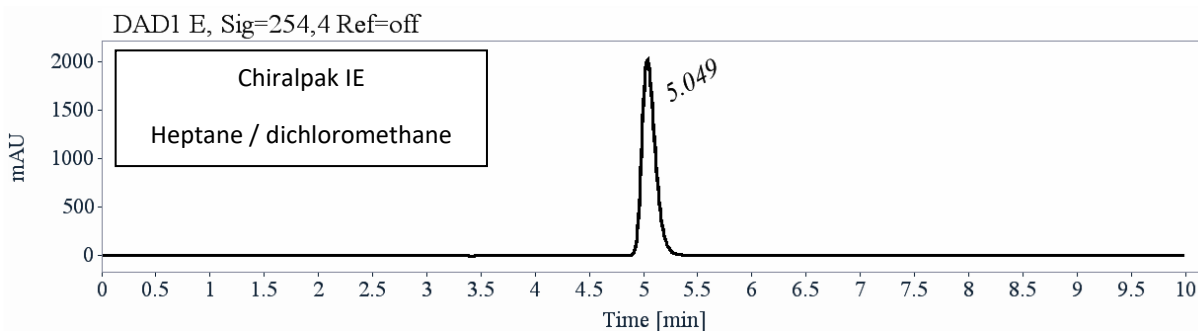
- The sample is dissolved in dichloromethane, injected on the chiral column, and detected with a UV detector at 254 nm and a circular dichroism detector at 254 nm. The flow-rate is 1 mL/min.

Column	Mobile Phase	t1	k1	t2	k2	α	Rs
Chiralpak IE	Heptane / dichloromethane (70/30)	5.05	0.71	6	1.03	1.45	3.85

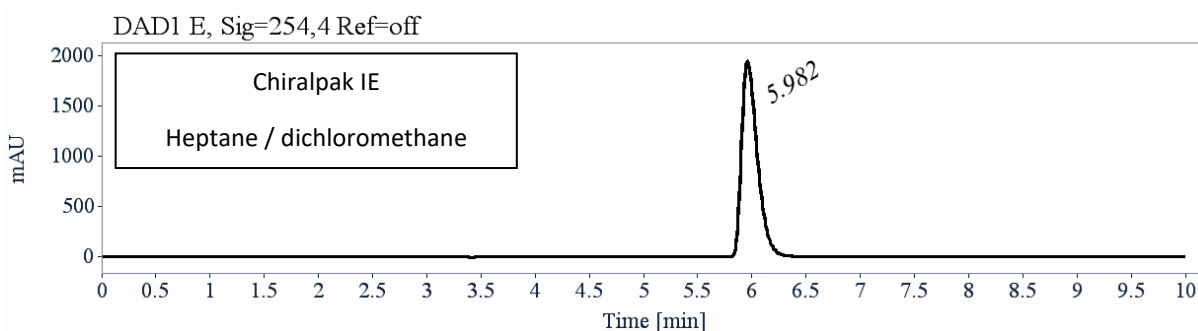


RT [min]	Area	Area%	Capacity Factor	Enantioselectivity	Resolution (USP)
5.05	9627	50.00	0.71		
6.00	9627	50.00	1.03	1.45	3.85
Sum	19254	100.00			

- Sample preparation: About 90 mg of compound **10** were dissolved in 4.25 mL of dichloromethane.
- Chromatographic conditions: Chiralpak IE (250 x 10 mm), hexane / dichloromethane (70/30) as mobile phase, flow-rate = 5 mL/min, UV detection at 254 nm.
- Injections (stacked): 85 times 50 μ L, every 6.7 minutes.
- First fraction: 40 mg of the first eluted with ee > 99.5 %



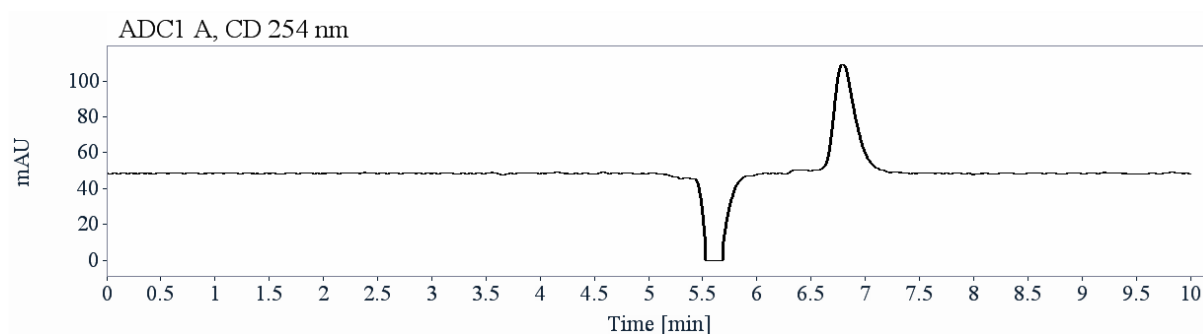
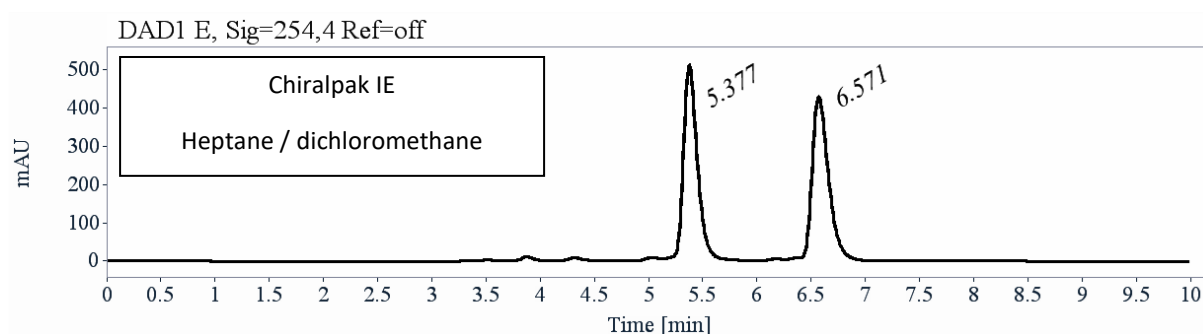
- Second fraction: 40 mg of the second eluted with ee > 99.5 %



Analytical chiral HPLC separation for compound **11**

- The sample is dissolved in dichloromethane, injected on the chiral column, and detected with a UV detector at 254 nm and a circular dichroism detector at 254 nm. The flow-rate is 1 mL/min.

Column	Mobile Phase	t1	k1	t2	k2	α	Rs
Chiralpak IE	Heptane / dichloromethane (70/30)	5.38 (-)	0.82	6.57 (+)	1.23	1.49	4.79

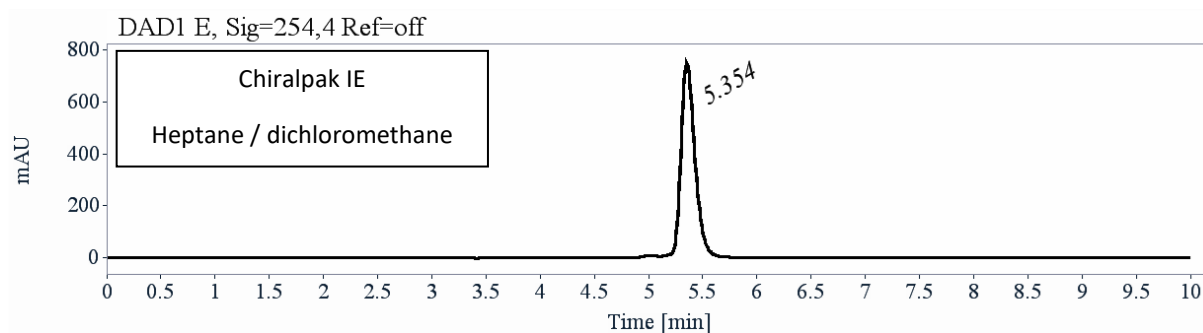


RT [min]	Area	Area%	Capacity Factor	Enantioselectivity	Resolution (USP)
5.38	4446	49.95	0.82		
6.57	4455	50.05	1.23	1.49	4.79
Sum	8900	100.00			

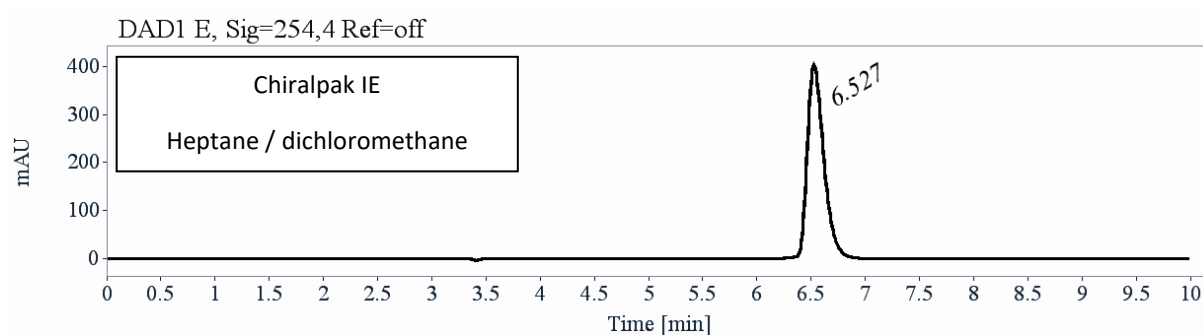
Preparative separation for compound **11**:

- Sample preparation: About 24 mg of compound **Endo-S2-H7** were dissolved in 5.2 mL of dichloromethane.
- Chromatographic conditions: Chiralpak IE (250 x 10 mm), hexane / dichloromethane (70/30) as mobile phase, flow-rate = 5 mL/min, UV detection at 254 nm.
- Injections (stacked): 35 times 150 μ L, every 7.5 minutes.

- First fraction: 5 mg of the first eluted with ee > 99.5 %

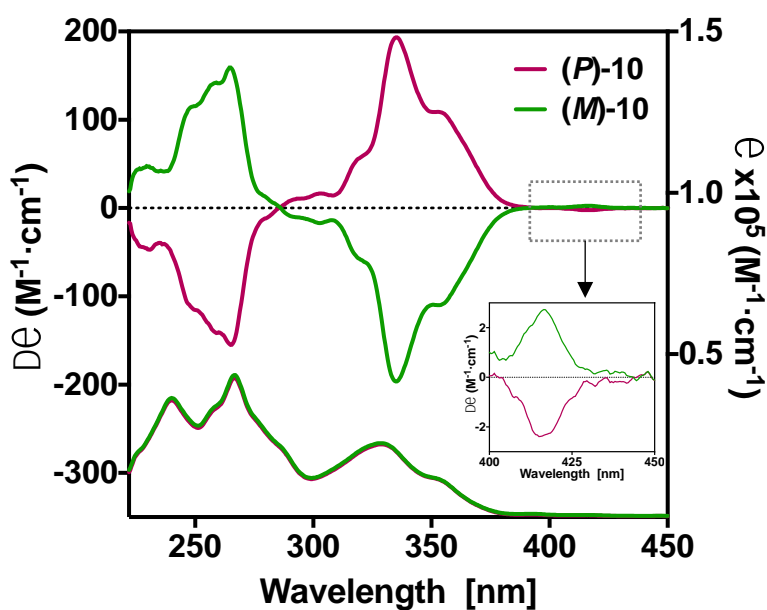
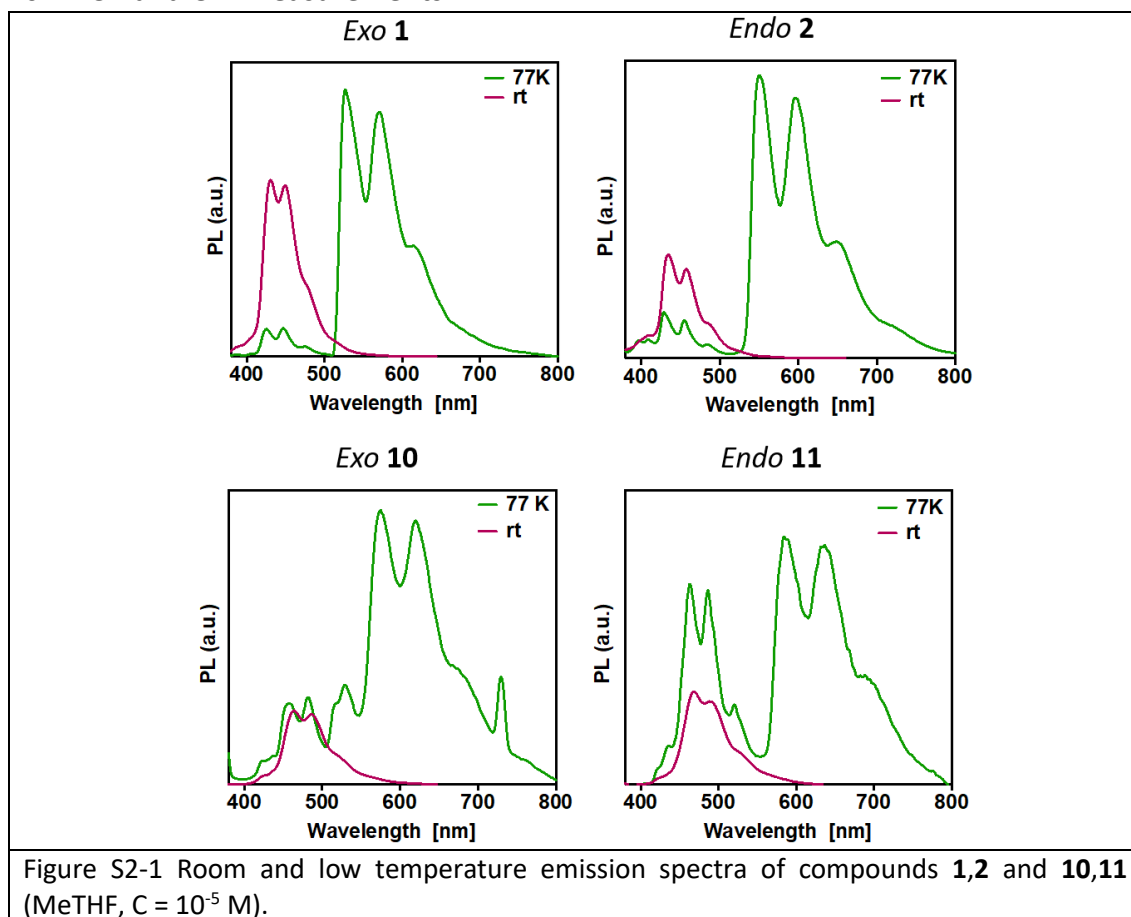


- Second fraction: 5 mg of the second eluted with ee > 99.5 %



10. Photophysical and chiroptical studies

10.1. CD and CPL measurements



11. Scanning Tunneling Microscopy (STM)

For general information and description of the methods used in STM imaging, refer to reference 14 in the main text. Additional graphic material is shown below.

Supplemental graphic material by STM

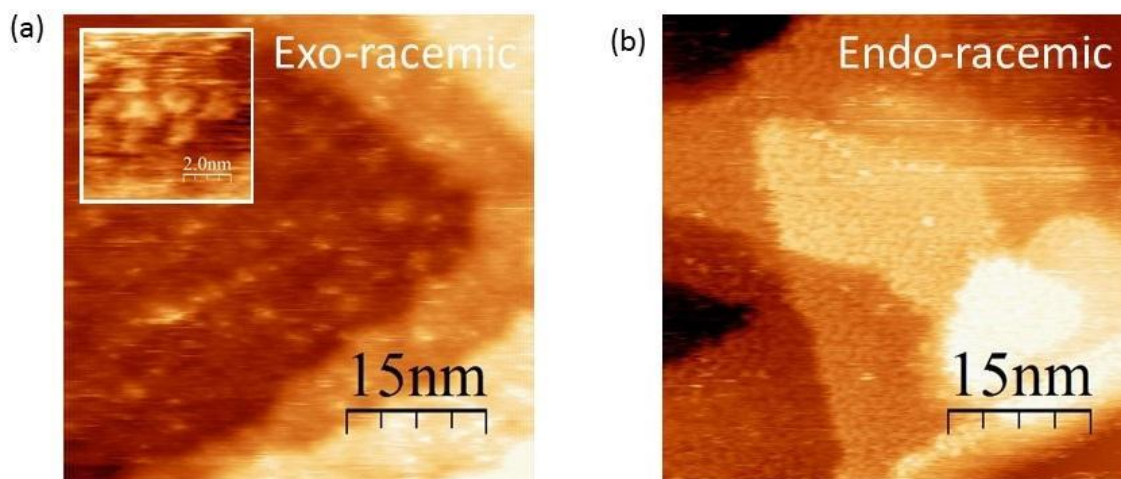


Figure S3. STM image of both topologies (a) *exo*- and (b) *endo*- dithia[9]helicenes racemic in benzene solution (in a concentration of $0.25 \text{ mg}\cdot\text{ml}^{-1}$) on (111)gold substrates deposited via drop casting. Set parameters are $V_{\text{bias}} = 0.5 \text{ V}$ and $I_t = 0.1 \times 10^{-9} \text{ A}$ for both panels whereas for the inset image are $V_{\text{bias}} = 0.4 \text{ V}$ and $I_t = 0.1 \times 10^{-9} \text{ A}$. No order is observed in either panel. Inset of panel (a) shows a zoom in of single molecules on gold substrates.

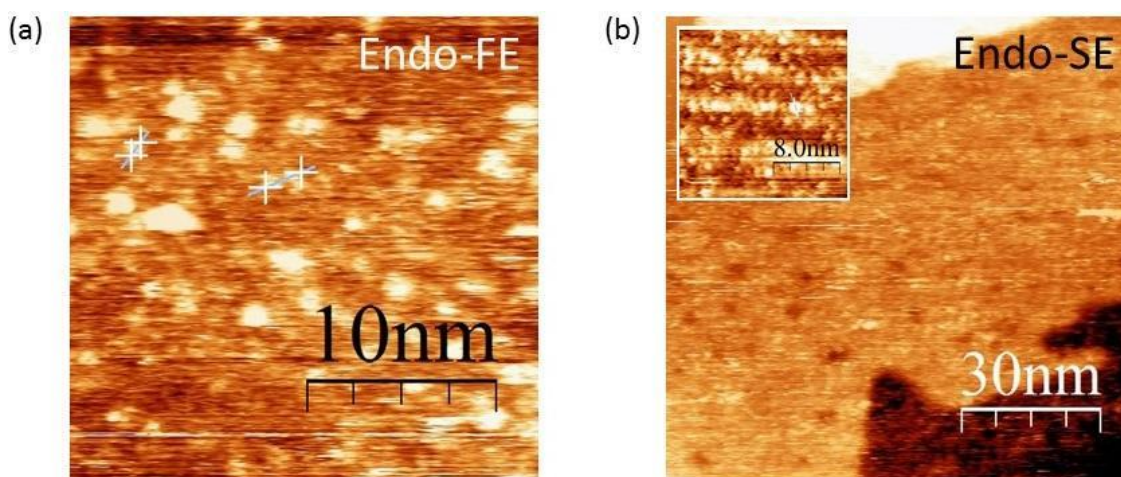


Figure S4. Topographic images of pure enantiomers of *endo*-dithia[9]helicene. Panel (a) shows the FE (first eluted = (+)-*P*) and (b) the SE (second eluted = (-)-*M*) enantiomer. Set parameters for panel (a) are $V_{\text{bias}} = -1.5 \text{ V}$ and $I_t = 0.1 \times 10^{-9} \text{ A}$ and for (b), $V_{\text{bias}} = 0.9 \text{ V}$ and $I_t = 0.1 \times 10^{-9} \text{ A}$. Inset of panel (b) shows the molecular distribution along the herringbone of the gold structure. For the inset case, the set parameters are $V_{\text{bias}} = 1.3 \text{ V}$ and $I_t = 0.03 \times 10^{-9} \text{ A}$.

Section S2: Theoretical part

1. Computational details.

All calculations were performed with Kohn–Sham density functional theory (KS DFT) and KS time-dependent DFT (TD-DFT) linear response methods. Geometry optimizations and vibrational frequency calculations with the CAM-B3LYP functional⁷ and the def2-SV(P) Gaussian-type basis set⁸ were performed with Gaussian 16, version A.03 (G16).⁹ S_1 equilibrium structures were optimized with excited state gradients from TD-DFT. Ground-state equilibrium structures were optimized with spin-restricted DFT. All structures were characterized as minima via harmonic vibrational frequency calculations. Calculations were performed with the (*P*) isomer of *exo*-dithia[9]helicene and *endo*-dithia[7]helicene, but the (*M*)-isomer was considered for comparison with the experimental data in the main text. Accordingly, the sign of the calculated chiroptical properties was inverted prior to reporting them in figures and tables.

Absorption and electronic circular dichroism (ECD) spectra were obtained considering the 30 lowest-lying excitations calculated using TD-DFT with the ground-state optimized geometries. The transitions were Gaussian broadened with a σ of 0.20 eV to obtain the corresponding spectra. Vibrationally resolved singlet emission and circularly polarized luminescence (CPL) spectra including Franck-Condon (FC) and Herzberg-Teller (HT) effects were calculated as implemented in G16.¹⁰ The vibronic transitions were Gaussian broadened with a σ of 0.0248 eV. Regarding general strategies for calculating natural optical activity parameters, in particular with DFT/TD-DFT, see, for example, References 11 and 12.

The CAM-B3LYP/def2-SV(P) level of theory yielded the correct signs for the ECD and CPL spectra except for the (*M*)-*exo*-dithia[7]helicene compound. Its ECD spectrum was investigated with a selection of functionals (M06-HF,¹³ M11,¹⁴ ω B97X-D,¹⁵ and LC- ω HPBE¹⁶) and the def2-SV(P) basis set, confirming that CAM-B3LYP predicts the correct ECD sign (**Figure S5**, Panels A and B). We chose the functionals listed above based on their known excellent performance for excitation energies.¹⁷ The ω B97X-D functional was used to re-optimize the S_0 and S_1 structures to obtain the vibrationally resolved CPL spectrum reported in **Figure S6**. The S_1 geometry obtained with this functional and basis set was then used as starting point in another geometry optimization with CAM-B3LYP. The optimized geometry obtained in this way was used to re-calculate the emission and CPL spectra, yielding the correct CPL sign as shown in **Figure S7**.

The dissymmetry factors (g_{lum}) reported in Table S7 were calculated as $\Delta I/I$, i.e. as the ratio between the broadened calculated CPL (ΔI) and emission (I) intensities at the experimental wavelengths, instead of using the rotatory and dipole strengths of the electronic transitions.¹⁸ This way was chosen because for the two dithia[9]helicenes the purely electronic spectrum of these compounds, unlike the experimental CPL band, has a positive rotatory strength for the S_0 - S_1 transition, whose contribution can still be observed as a weak feature around the wavelength of the 0-0 transition in the vibrationally resolved calculated CPL spectrum for the *exo* isomer (**Figure S11**). To further investigate the origin of this negative band, calculations were performed for the FC and HT intensities separately from each other. The experimental spectra shown in **Figure S16** were arbitrarily scaled to match the calculated intensities.¹⁸

It has been reported that HT effects heavily influence the shape and sign of ECD and CPL spectra for [6]helicene and its 2-methyl-, 5-aza-, and 2-bromo-derivatives through the modification of

the FC spectral features.¹⁸ As revealed by the present calculations, this is also the case for (*M*)-*exo*-dithia[7]helicene and the two dithia[9]helicenes. For the first compound, the FC spectrum already reproduces the shape and sign of the experimental equivalent well, although the relative intensity of the two experimental bands around 430 and 450 nm is not correctly reproduced. The experimental spectrum shows two bands of roughly the same intensity. The calculated FC spectrum, instead, shows two peaks of different intensity, with the first band being more intense than the second. HT effects alone are not enough to obtain a satisfactory agreement with the experiment. The combined FCHT spectrum appears less intense than the one including FC effects only due to FC and HT spectra having opposite signs. This reduces the intensity of both bands in the 430–450 nm range by roughly the same amount (panel A of **Figure S16**).

The CPL spectrum obtained including only FC contributions for the two [9]helicenes exhibits the wrong sign. For (*M*)-*endo*-dithia[9]helicene, the intensity of the FC spectrum is very weak in the whole spectral range, and the HT spectrum accounts for most of the spectral shape. The experimental spectrum is overall not well resolved, showing a major negative band whose intensity is largest around 460–470 nm. Individual bands are not clearly visible, instead. The computed HT and FCHT spectra exhibit the same pattern, with the most intense peak around 470 nm accompanied by two less intense shoulders. The FC spectrum of (*M*)-*exo*-dithia[9]helicene is opposite in sign to the HT spectrum, as for the (*M*)-*endo*-dithia[9]helicene compound. HT effects are responsible for the satisfactory agreement with the experimental data exhibited by the HT and FCHT spectra. The experimental spectrum shows three maxima, although not well resolved, that are matched by the calculated pattern. FC effects are responsible for the positive band observed between 450 and 460 nm, while the sign change is due to HT effects.

Overall, HT effects are responsible for sign changes, relative to the purely electronic spectra, for the calculated CPL of some of the systems. In addition, the simultaneous inclusion of FC and HT effects is necessary to obtain satisfactory agreement with the experimental data, similar to what was shown previously for hexahelicene and its derivatives in reference 18. As discussed in the main text, this is partially due to small rotatory strengths for the S_1 – S_0 transition of these compounds, reported in **Tables S1–S3** below.

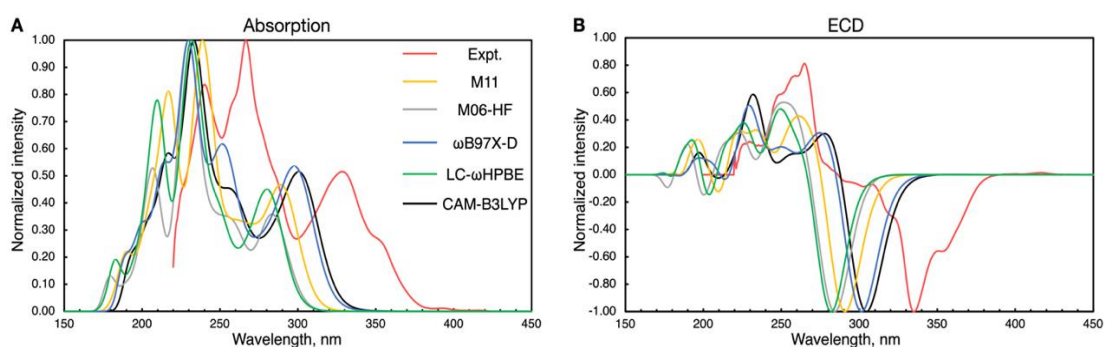


Figure S5 Normalized absorption (Panel **A**) and ECD (Panel **B**) spectra calculated with the CAM-B3LYP, LC- ω HPBE, M11, M06-HF, ω B97X-D functionals and the def2-SV(P) basis set on CAM-B3LYP/def2-SV(P) optimized geometries of (*M*)-*exo*-dithia[7]helicene. A Gaussian broadening with $\sigma = 0.20$ eV was applied to the transitions. Calculated spectra are unshifted.

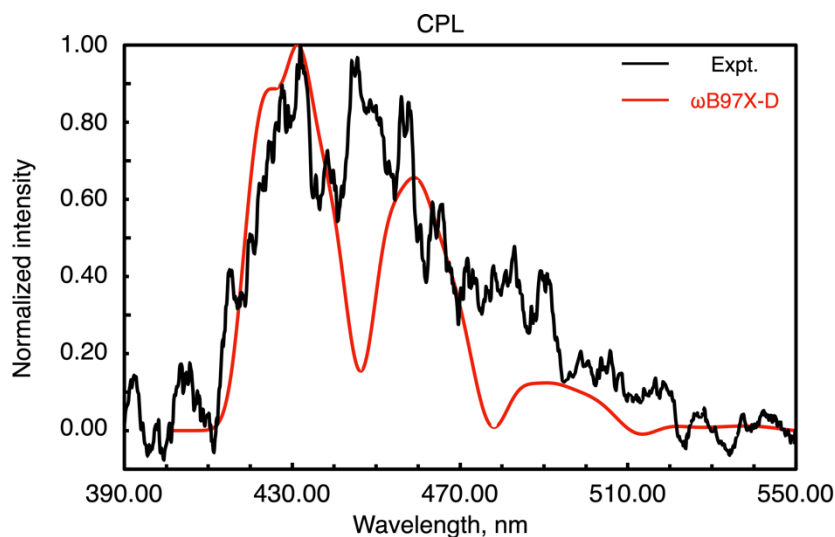


Figure S6 Normalized CPL spectrum for (*M*)-*exo*-dithia[7]helicene obtained with ω B97X-D/def2-SV(P). A Gaussian broadening with $\sigma = 0.0248$ eV was applied. A shift of -0.40 eV was applied to the computed spectrum.

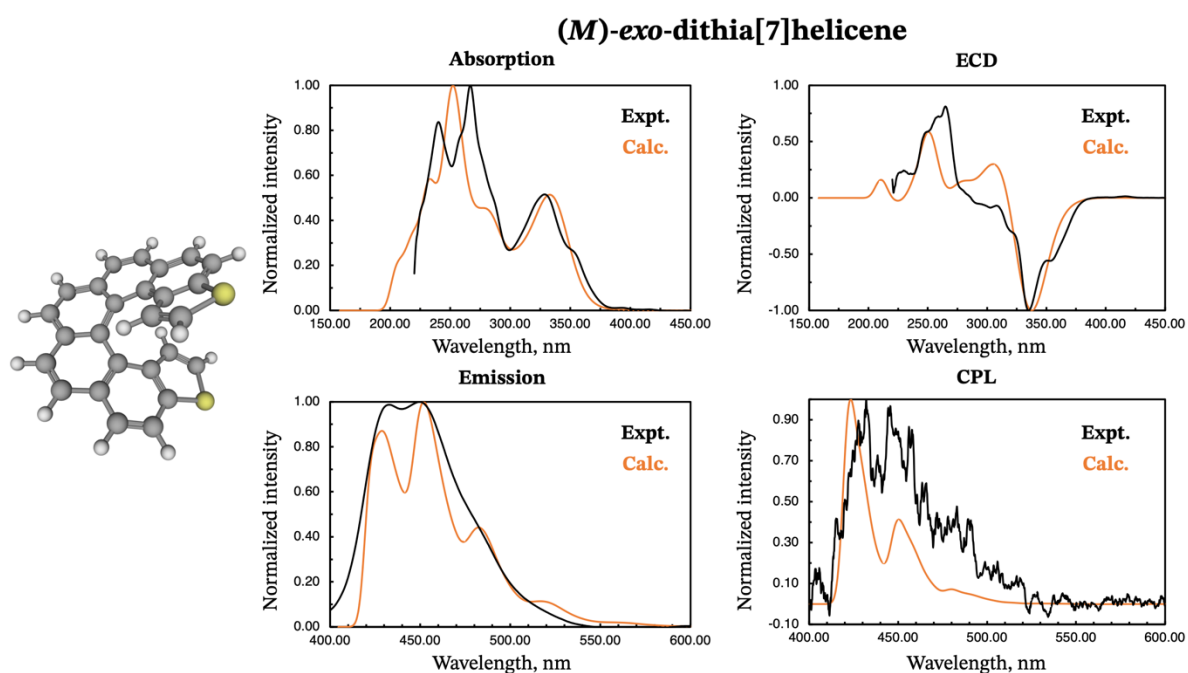


Figure S7 Normalized absorption, ECD, vibrationaly resolved singlet emission and CPL spectra alongside the optimized ground state structure of (*M*)-*exo*-dithia[7]helicene obtained with CAM-B3LYP/def2-SV(P). Calculated spectra were shifted by -0.40 eV (orange curves). Hydrogen atoms are white, carbon atoms are black, sulfur atoms are yellow.

Table S1 Twenty lowest excitation energies, oscillator strengths, rotatory strengths, and orbital contributions for the transitions (greater than 15.0 %) of (*M*)-*exo*-dithia[7]helicene. The values in parentheses are rotatory strengths calculated for the S_1-S_0 transition (on the S_1 geometry).

Excitation number	Excitation energy ^a	Wavelength ^b	Oscillator strength ^c	Rotatory strength ^d	Occupied orbital	Virtual orbital	Percentage ^e
1	3.594	345	0.0012	3.61 (5.89)	100	103	34.6%
					101	102	53.3%
2	3.834	323	0.0065	-28.17 (-30.00)	100	102	56.7%
					101	103	36.7%
3	4.087	303	0.3564	-904.80 (-878.67)	100	102	31.7%
					101	103	45.7%
4	4.228	293	0.0046	-30.09 (-7.60)	98	102	34.8%
					99	103	25.0%
					101	105	17.2%
5	4.293	289	0.1390	191.46 (322.26)	99	102	38.0%
					101	102	20.3%
6	4.483	277	0.1158	175.55 (40.20)	99	102	29.1%
					100	103	45.8%
					101	102	19.4%
7	4.740	262	0.1935	5.97 (-3.36)	98	102	29.5%
					99	103	48.7%
8	4.844	256	0.1243	99.51 (90.36)	98	103	36.4%
					99	102	24.5%

					100	105	24.1%
9	4.955	250	0.0403	-9.31 (-12.01)	98	105	15.9%
					99	104	22.4%
					101	104	18.9%
10	5.041	246	0.0848	6.18 (-2.94)	98	102	18.8%
					99	105	20.7%
					100	104	23.5%
11	5.043	246	0.0328	41.75 (46.36)	98	103	33.4%
					101	104	32.2%
12	5.096	243	0.0866	-69.98 (-79.81)	101	105	60.4%
13	5.235	237	0.1009	0.58 (9.66)	97	102	26.8%
					100	104	44.7%
14	5.327	233	0.6304	372.46 (411.10)	100	105	51.2%
					101	104	24.0%
15	5.438	228	0.0294	13.46 (26.48)	97	102	27.5%
					99	105	40.7%
16	5.497	226	0.0057	-15.61 (15.66)	96	102	25.0%
					99	104	45.8%
17	5.553	223	0.1254	47.29 (31.13)	96	103	24.8%
18	5.567	223	0.0017	27.79 (-51.13)	97	103	62.2%

					98	105	20.8%
19	5.747	216	0.2113	226.84 (251.78)	96	102	25.7%
					98	105	46.4%
20	5.754	215	0.1756	-234.34 (-247.23)	96	103	25.2%
					98	104	39.1%

^aIn units of eV; ^bIn units of nm; ^cDimensionless; ^dIn units of 10^{-40} esu² cm²;

^eCalculated using the square of the coefficients printed by the G16 program.

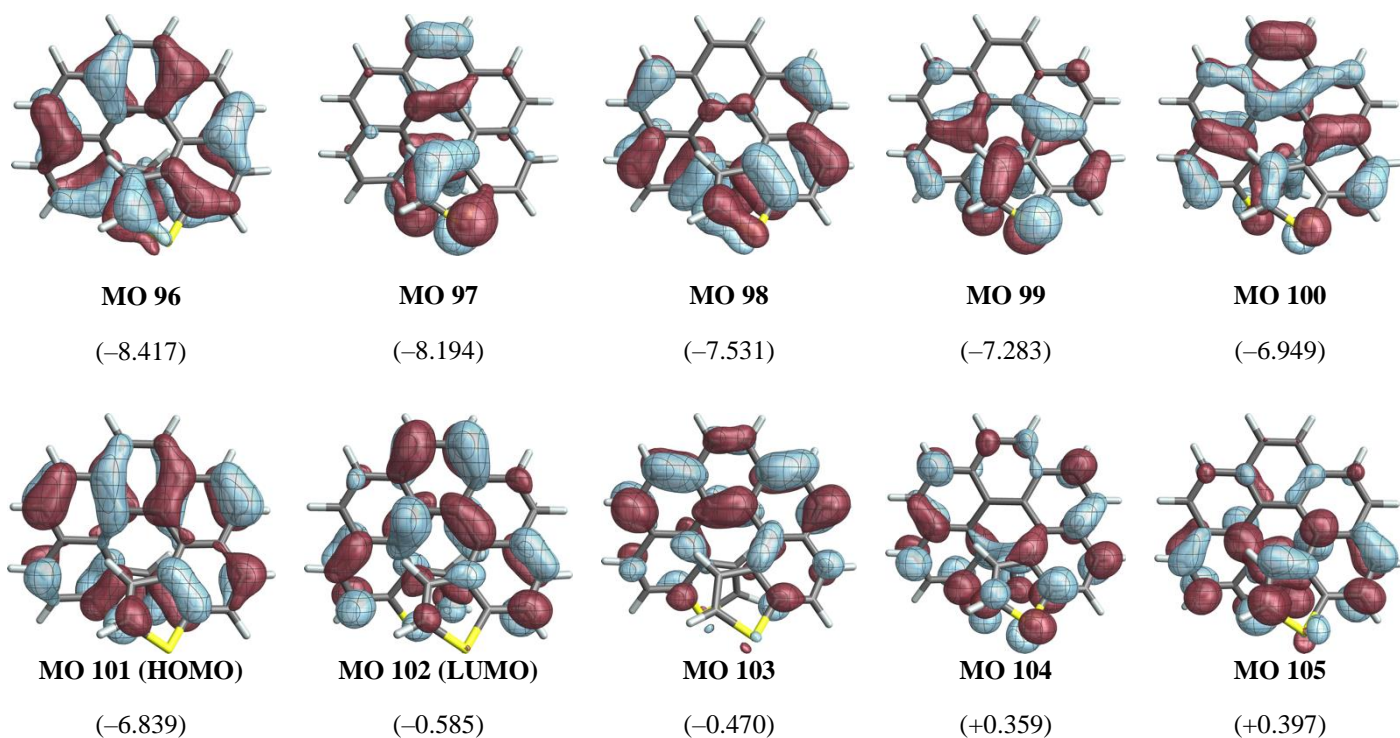


Figure S8 Molecular orbitals involved in the excitations for (*M*)-*exo*-dithia[7]helicene. Values in parentheses are orbital energies in eV. Iso values ± 0.030 a.u., ground state geometry.

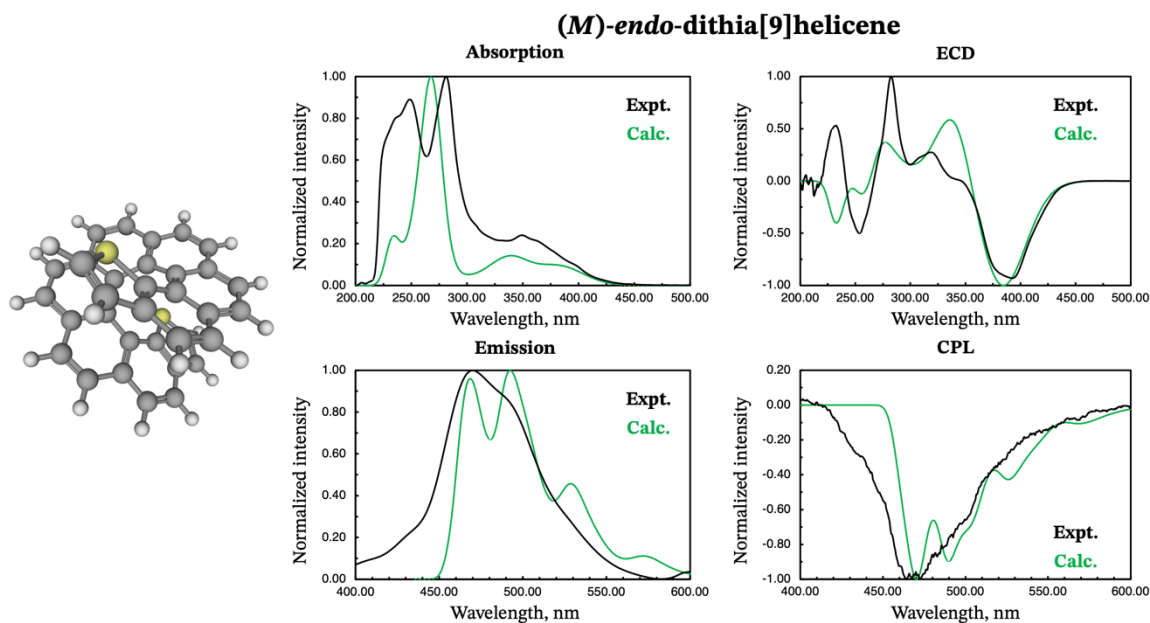


Figure S9 Normalized absorption, ECD, vibrationally resolved singlet emission and CPL spectra alongside the optimized ground state structure of (*M*)-*endo*-dithia[9]helicene obtained with CAM-B3LYP/def2-SV(P). Calculated spectra were shifted by -0.40 eV (green curves). Hydrogen atoms are white, carbon atoms are black, sulfur atoms are yellow.

Table S2 Twenty lowest excitation energies, oscillator strengths, rotatory strengths, and orbital contributions for the transitions (greater than 15.0 %) of (*M*)-*endo*-dithia[9]helicene. The values in parentheses are rotatory strengths calculated for the S_1-S_0 transition (on the S_1 geometry).

Excitation number	Excitation energy ^a	Wavelength ^b	Oscillator strength ^c	Rotatory strength ^d	Occupied orbital	Virtual orbital	Percentage ^e
1	3.364	369	0.0001	0.20 (0.21)	126	128	32.8%
					127	129	48.4%
2	3.534	351	0.0492	-433.79 (-399.67)	127	128	84.0%
					125	128	29.6%
3	3.652	340	0.0630	-584.39 (-741.53)	126	129	55.8%
					124	129	42.0%
4	3.817	325	0.0529	-244.22 (-56.83)	125	128	19.6%
					124	128	19.3%
5	3.915	317	0.0015	7.92 (2.39)	125	129	56.1%
					126	128	53.5%
6	4.026	308	0.1342	487.33 (372.31)	127	129	34.8%
					124	128	44.6%
7	4.210	295	0.0015	17.33 (152.41)	125	129	22.5%
					124	129	34.0%
8	4.219	294	0.0750	160.26 (148.47)	125	128	33.9%
					126	129	16.4%
9	4.363	284	0.0226	35.77 (14.13)	122	129	18.1%

					123	128	18.9%
					125	130	19.8%
10	4.527	274	0.0198	38.52 (46.06)	124	128	15.8%
					127	130	67.2%
11	4.557	272	0.0107	3.37 (12.26)	122	128	18.5%
					123	129	42.0%
12	4.589	270	0.0088	21.72 (3.74)	124	129	16.4%
					126	130	17.6%
					127	131	36.4%
13	4.750	261	0.0129	72.65 (112.08)	125	131	31.7%
14	4.801	258	0.0002	6.87 (101.54)	123	128	39.5%
					124	131	32.1%
15	4.824	257	0.0145	81.65 (-8.44)	122	129	17.3%
					125	130	45.0%
16	4.843	256	0.0317	-11.81 (11.09)	122	128	20.1%
					124	130	17.4%
					126	130	23.6%
					127	131	25.0%
17	4.993	248	0.3515	272.04 (228.68)	122	128	23.0%
					123	129	25.3%
18	4.997	248	0.4663	211.35 (258.32)	122	129	39.6%

					123	128	16.0%
19	5.022	247	0.0841	-133.94 (-169.21)	124	131	27.8%
					126	131	32.0%
20	5.040	246	0.2230	-203.58 (-161.17)	124	130	33.9%
					125	131	19.0%
					126	130	18.3%

^aIn units of eV; ^bIn units of nm; ^cDimensionless; ^dIn units of 10^{-40} esu² cm²;

^eCalculated using the square of the coefficients printed by the G16 program.

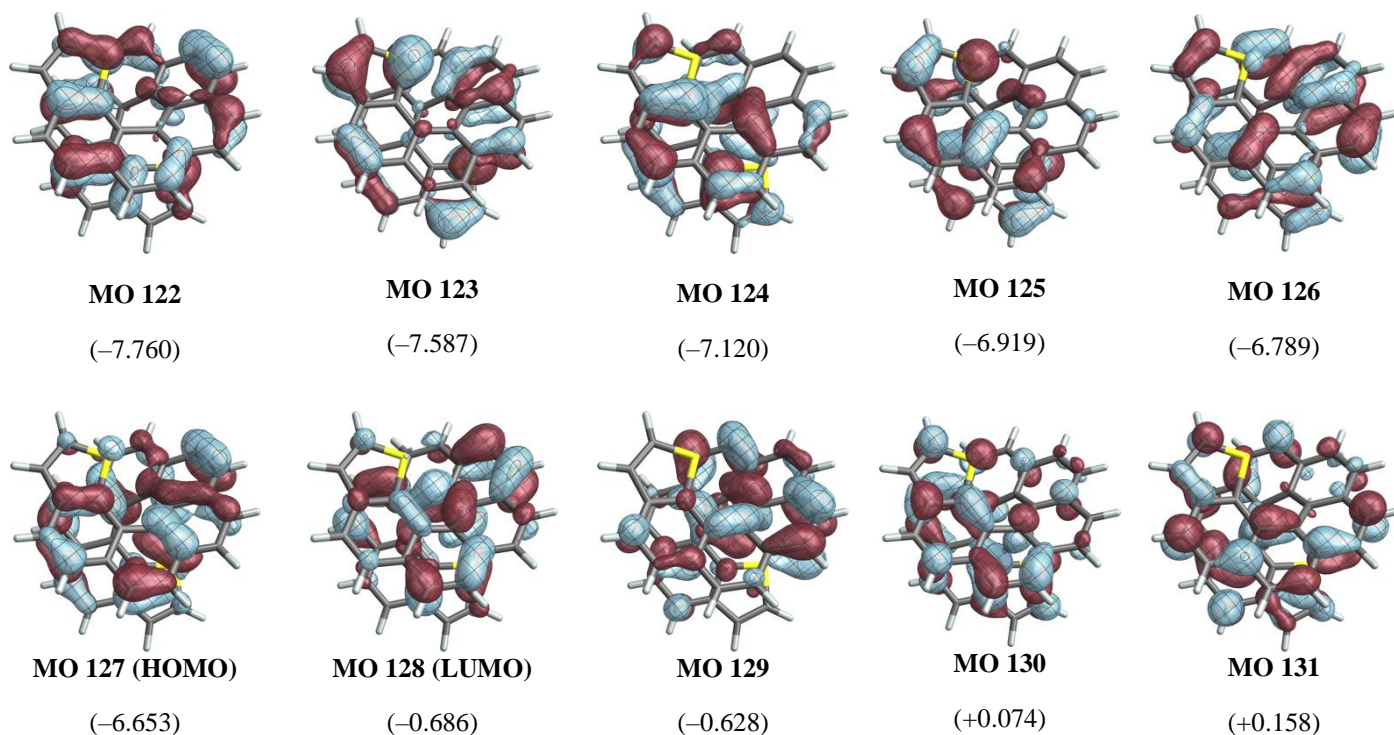


Figure S10 Molecular orbitals involved in the excitations for (*M*)-*endo*-dithia[9]helicene. Values in parentheses are orbital energies in eV. Iso values ± 0.030 a.u., ground state geometry.

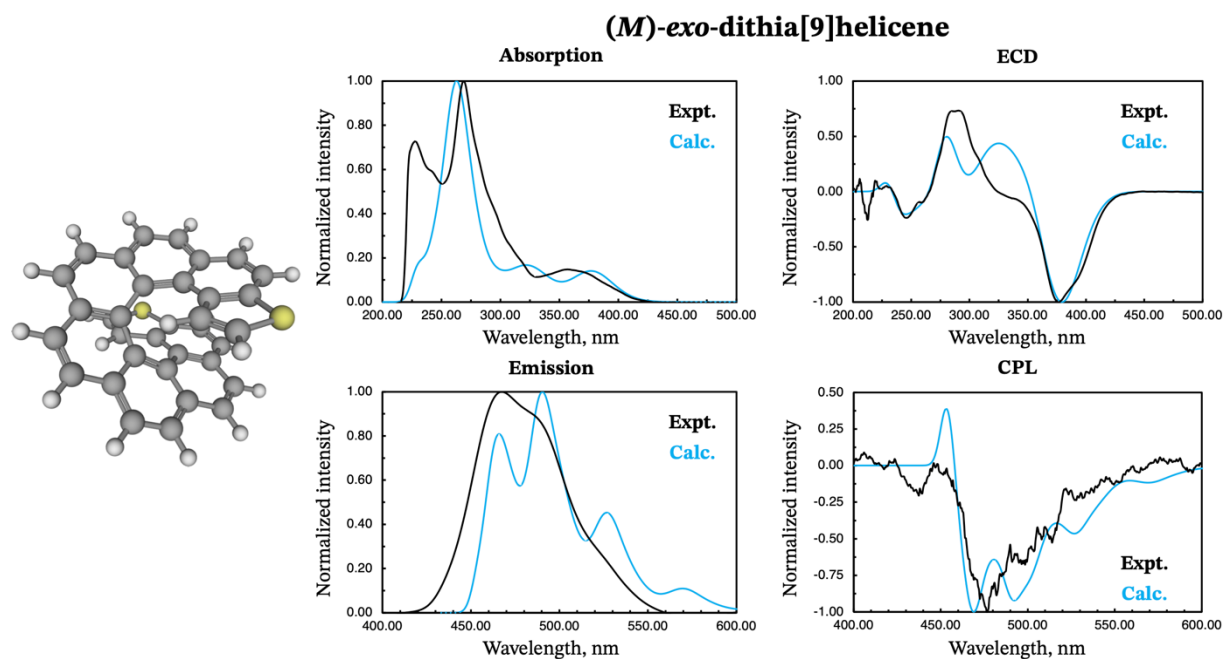


Figure S11 Normalized absorption, ECD, vibrationaly resolved singlet emission and CPL spectra alongside the ground state structure of (*M*)-exo-dithia[9]helicene obtained with CAM-B3LYP/def2-SV(P). Calculations were performed with the (*P*) isomer. The sign of the ECD and CPL spectra and the optimized geometry were inverted. Calculated spectra were shifted by -0.40 eV (blue curves). Hydrogen atoms are white, carbon atoms are black, sulfur atoms are yellow.

Table S3 Twenty lowest excitation energies, oscillator strengths, rotatory strengths, and orbital contributions for the transitions (greater than 15.0 %) of (*M*)-exo-dithia[9]helicene. Calculations were performed with the (*P*) isomer, the sign of the rotatory strength was inverted for the (*M*) enantiomer. The values in parentheses are rotatory strengths calculated for the S_1-S_0 transition (on the S_1 geometry).

Excitation number	Excitation energy ^a	Wavelength ^b	Oscillator strength ^c	Rotatory strength ^d	Occupied orbital	Virtual orbital	Percentage ^e
1	3.384	366	0.0002	2.52 (3.13)	126	129	32.9%
					127	128	47.7%
2	3.597	345	0.0081	-22.40 (4.59)	126	128	27.9%
					127	129	60.4%
3	3.677	337	0.1460	-1180.00 (-1112.06)	126	128	56.9%
					127	129	18.9%
4	3.842	323	0.0019	3.40	124	128	34.3%

				(2.76)			
					125	129	32.3%
5	3.908	317	0.0339	140.03 (239.19)	125	128	33.7%
					127	128	30.3%
6	4.125	301	0.0978	254.27 (87.22)	126	129	51.7%
					127	128	17.1%
7	4.275	290	0.0733	125.50 (104.77)	124	128	31.6%
					125	129	42.0%
8	4.346	285	0.0536	161.48 (188.31)	124	129	56.7%
					125	128	32.3%
9	4.442	279	0.0157	3.11 (2.26)	122	128	15.9%
					124	131	22.7%
					125	130	24.8%
10	4.564	272	0.0100	-15.85 (-44.57)	126	131	23.3%
					127	130	52.3%
11	4.568	271	0.0256	33.73 (-3.62)	125	131	25.3%
12	4.590	270	0.0633	-23.62 47.20)	127	131	49.4%
13	4.794	259	0.0443	60.63 (107.44)	123	128	24.7%
					124	130	18.2%
					126	130	15.6%
14	4.837	256	0.1638	383.84	124	131	25.1%

				(419.90)			
					126	131	34.4%
					127	130	15.0%
15	4.881	254	0.0014	-13.78 (-24.29)	122	128	26.0%
					123	129	21.7%
					125	130	34.8%
16	4.900	253	0.0677	68.05 (19.17)	125	131	30.3%
					126	130	37.4%
17	5.005	248	0.0777	27.12 (115.52)	123	128	38.0%
					125	131	22.1%
18	5.020	247	0.2650	-218.70 (1.61)	123	129	15.9%
					124	131	18.6%
					126	131	26.2%
					127	130	16.9%
19	5.081	244	0.1872	213.87 (0.43)	122	128	39.7%
					123	129	30.8%
					124	131	18.2%
20	5.129	242	0.2593	-212.97 (27.70)	124	130	42.8%

^aIn units of eV; ^bIn units of nm; ^cDimensionless; ^dIn units of 10^{-40} esu² cm²;

^eCalculated using the square of the coefficients printed by the G16 program.

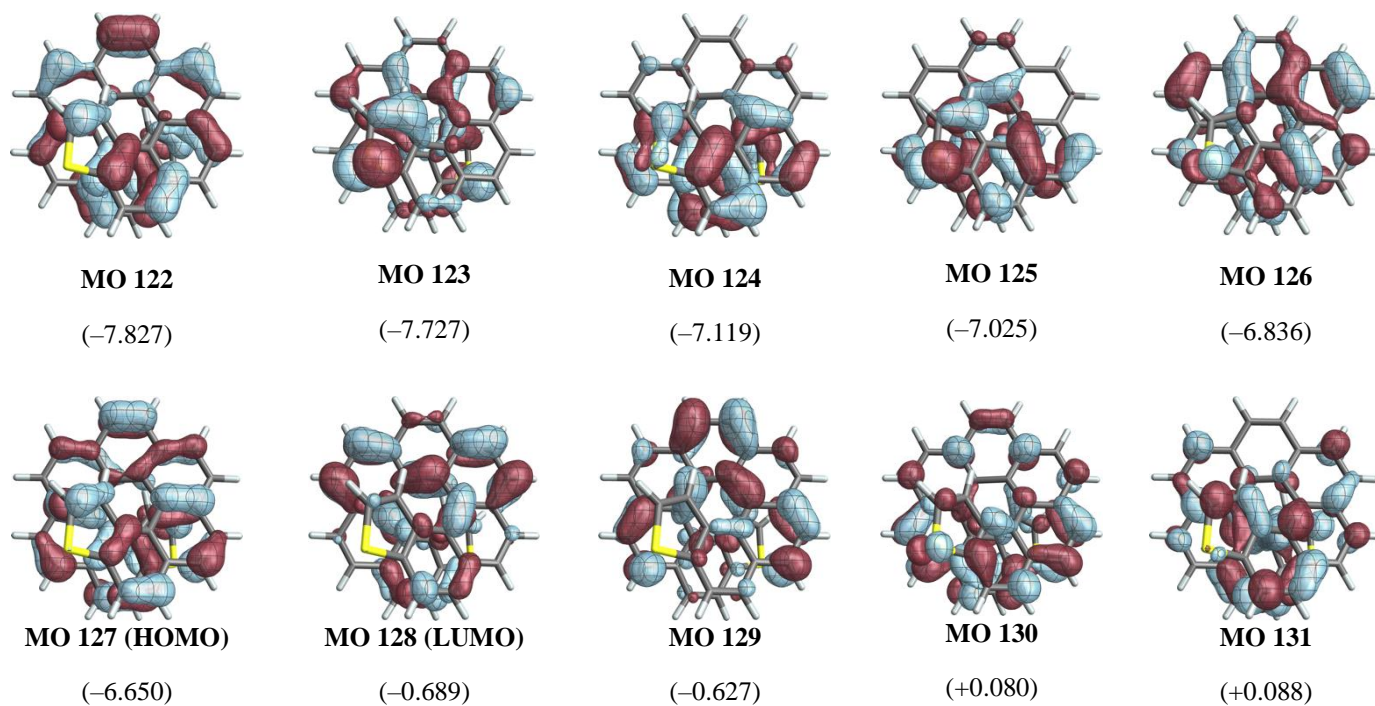


Figure S12 Molecular orbitals involved in the excitations for (*M*)-*exo*-dithia[9]helicene. Values in parentheses are orbital energies in eV. Iso values ± 0.030 a.u., ground state geometry calculated with the (*P*) isomer and subsequently inverted.

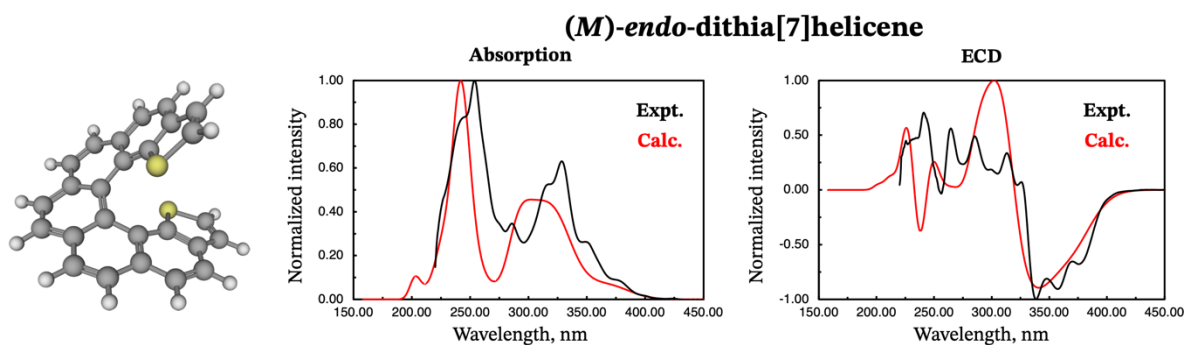


Figure S13 Normalized absorption and ECD spectra alongside the optimized ground state structure of (*M*)-*endo*-dithia[7]helicene obtained with CAM-B3LYP/def2-SV(P). Calculations were performed with the (*P*) isomer. The sign of the ECD spectrum and the optimized geometry were inverted. Calculated spectra were shifted by -0.40 eV (red curves). Hydrogen atoms are white, carbon atoms are black, sulfur atoms are yellow.

Table S4 Twenty lowest excitation energies, oscillator strengths, rotatory strengths, and orbital contributions for the transitions (greater than 15.0 %) of (*M*)-*endo*-dithia[7]helicene. Calculations were performed with the (*P*) isomer, the sign of the rotatory strength was inverted for the (*M*) enantiomer.

Excitation number	Excitation energy ^a	Wavelength ^b	Oscillator strength ^c	Rotatory strength ^d	Occupied orbital	Virtual orbital	Percentage ^e
1	3.548	349	0.0011	-1.87	100	102	38.8%
					101	103	51.3%
2	3.730	332	0.0525	-258.66	101	102	80.3%
3	3.967	313	0.0533	-334.17	99	102	50.5%
					100	103	35.4%
4	4.196	296	0.2680	-411.72	98	103	28.1%
					100	103	35.4%
5	4.241	292	0.0101	20.72	98	102	15.6%
					99	103	62.5%
6	4.401	282	0.2757	493.59	100	102	45.4%
					101	103	40.6%
7	4.615	269	0.2020	26.07	98	103	43.6%
					99	102	24.5%
8	4.669	266	0.1603	303.15	98	102	58.9%
					99	103	26.0%
9	4.881	254	0.0173	-57.68	96	103	16.0%

					97	102	34.3%
					99	104	23.3%
10	5.065	245	0.0345	48.63	101	104	69.3%
11	5.113	243	0.0030	-5.85	97	103	56.9%
12	5.170	240	0.0258	-5.34	98	103	20.6%
					100	104	17.9%
					101	105	42.7%
13	5.306	234	0.0283	-61.75	97	102	50.5%
					98	105	15.8%
14	5.317	233	0.0799	-9.51	96	102	23.8%
					99	105	15.4%
					100	104	37.4%
15	5.448	228	0.2459	410.02	99	104	36.2%
					100	105	38.9%
16	5.464	227	0.0854	-1.56	97	103	23.8%
					99	105	33.5%
17	5.540	224	0.4434	-255.44	96	102	25.1%
					100	104	22.9%
					101	105	23.9%
18	5.596	222	0.2679	-191.57	96	103	27.8%
					99	104	15.5%
					100	105	30.9%
19	5.791	214	0.0500	-72.18	98	104	61.4%
					99	105	17.1%
20	5.841	212	0.1786	333.58	96	103	19.3%
					98	105	47.0%

^aIn units of eV; ^bIn units of nm; ^cDimensionless; ^dIn units of 10^{-40} esu² cm²;

^eCalculated using the square of the coefficients printed by the G16 program.

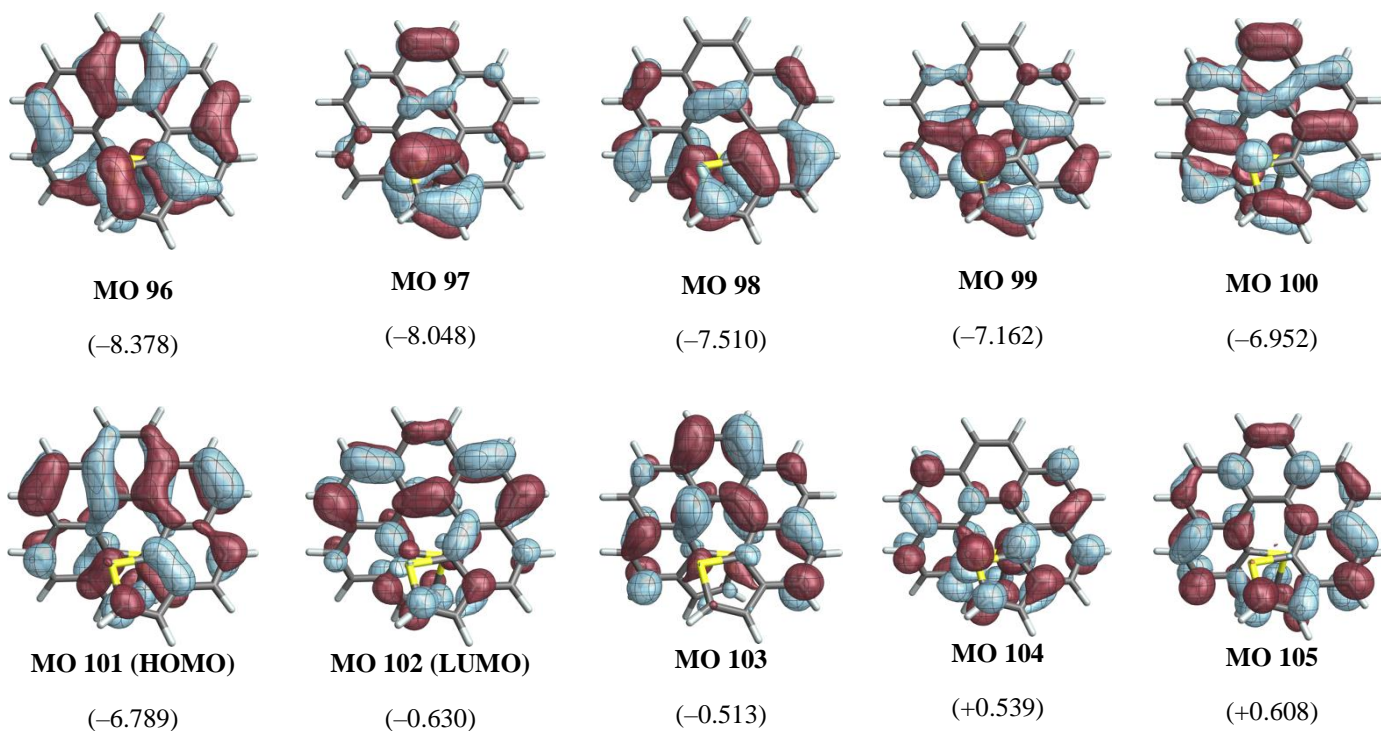


Figure S14 Molecular orbitals involved in the excitations for (*M*)-endo-dithia[7]helicene. Values in parentheses are orbital energies in eV. Iso values ± 0.030 a.u., ground state geometry calculated with the (*P*) isomer and subsequently inverted.

Table S7 Experimental and calculated dissymmetry factors (g_{LUM}) for (*M*)-exo-dithia[7]helicene, (*M*)-endo-dithia[9]helicene, and (*M*)-exo-dithia[9]helicene.

Compound	$g_{\text{LUM, expt}}^a$	Expt. wavelength ^b	$g_{\text{LUM, calc}}^{a,c}$	Calc. wavelength ^{b,d}	Excitation energy ^e	Excitation energy, shifted ^e
(<i>M</i>)-exo-thia-heptahelicene	0.005	470	0.0024	470.0	3.04	2.64
(<i>M</i>)-endo-thia-nonahelicene	-0.0123	470	-0.024	470.4	3.04	2.64
(<i>M</i>)-exo-thia-nonahelicene	-0.0042	475	-0.019 ^f	469.0	3.04	2.64

^aDimensionless; ^bIn nm; ^cCalculated as Δ/I at the wavelengths given in column 5 (see text); ^dAfter shifting; ^eIn eV;

^fAfter sign change from the calculations with the (*P*) enantiomer.

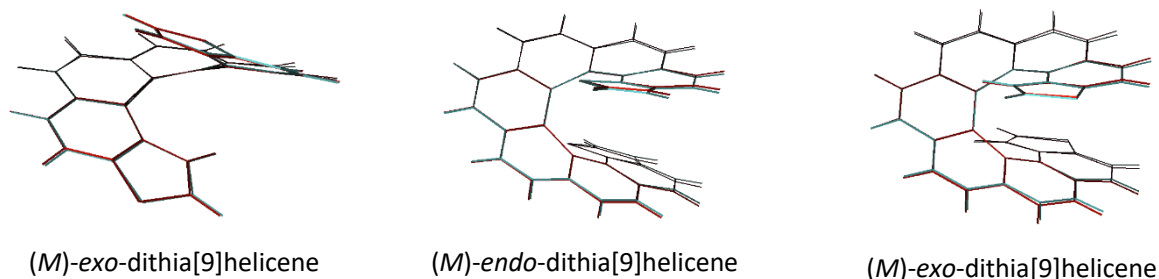


Figure S15 Optimized S_0 (red) and S_1 (blue) geometries superimposed with one another for (*M*)-exo-thia-heptahelicene (left), (*M*)-endo-thia-nonahelicene (middle), and (*M*)-exo-thia-nonahelicene (right).

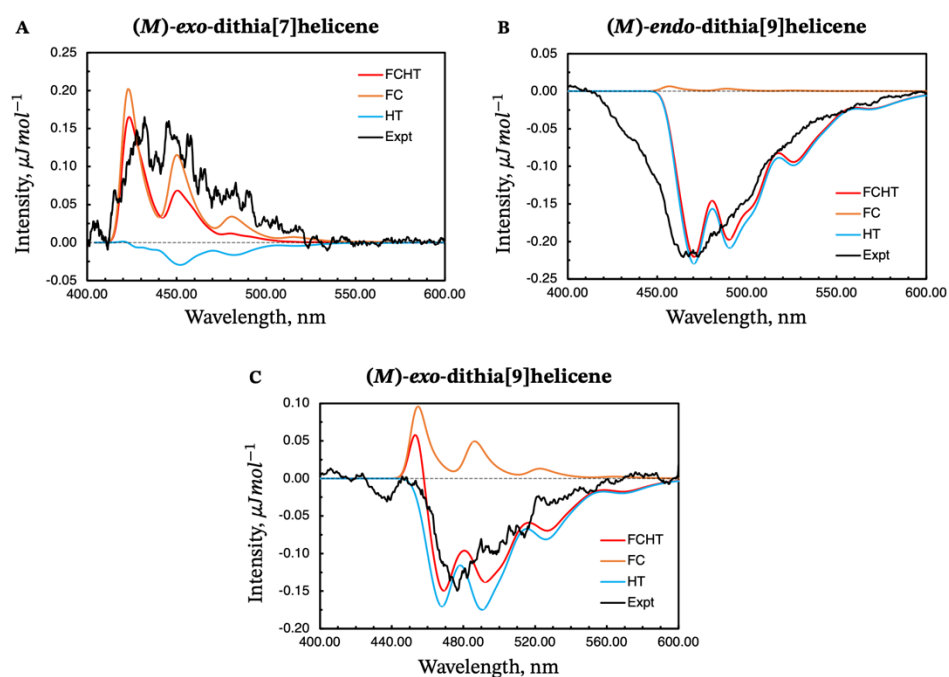


Figure S16 Calculated CPL spectra including Franck-Condon (FC, orange lines), Herzberg-Teller (HT, blue lines), and FCHT effects (red lines) compared to the experimental spectra for (*M*)-exo-dithia[7]helicene (top left, panel A), (*M*)-endo-dithia[9]helicene (top right, panel B), and (*M*)-exo-dithia[9]helicene (bottom, panel C; calculations were performed with (*P*)-exo-dithia[9]helicene and the sign of the CPL spectra was inverted). Calculated spectra are Gaussian broadened ($\sigma = 0.0248$ eV) and shifted by -0.40 eV. Experimental spectra were scaled to match the calculated intensities.

Table S8 Vibrational normal modes implied in the most intense vibronic transitions for the *M* isomers of *exo*-dithia[7]helicene, *endo*-dithia[9]helicene, and *exo*-dithia[9]helicene. The numbering follows the G16 output.

Molecule	Normal modes #	Wavenumber (cm ⁻¹)
<i>(M)</i> - <i>exo</i> -dithia[7]helicene	2	56
	4	97
	9	215
	15	338
	89	1428
	92	1455
<i>(M)</i> - <i>endo</i> -dithia[9]helicene	3	54
	11	154
	19	312
	22	370
	25	428
	42	630
	113	1421
	115	1428
	121	1467
128	1584	
<i>(M)</i> - <i>exo</i> -dithia[9]helicene	3	55
	7	107
	25	421
	42	631
	115	1426
	117	1437
	119	1453
	120	1453
	128	1593
133	1676	

(M)-exo-dithia[7]helicene

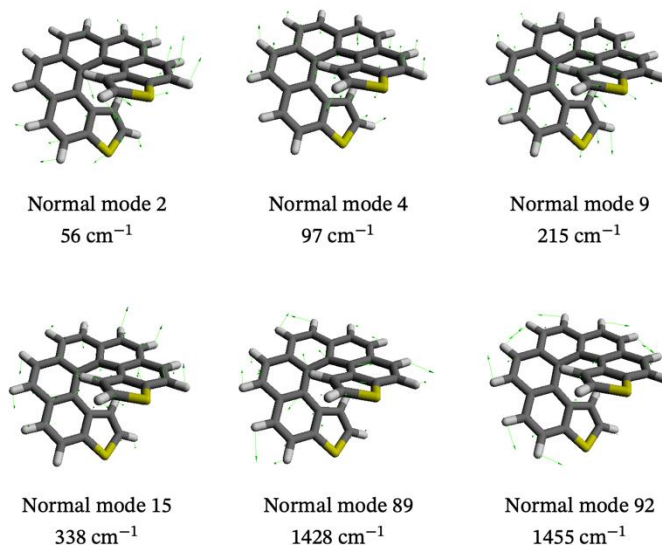


Figure S17 Selected vibrational normal modes for (M)-exo-dithia[7]helicene related to the most intense vibronic peaks in the calculated CPL spectra. The green vectors indicate the direction of the displacement for the corresponding frequency (in cm⁻¹). The numbers refer to the order the normal modes appear in the G16 output.

(M)-endo-dithia[9]helicene

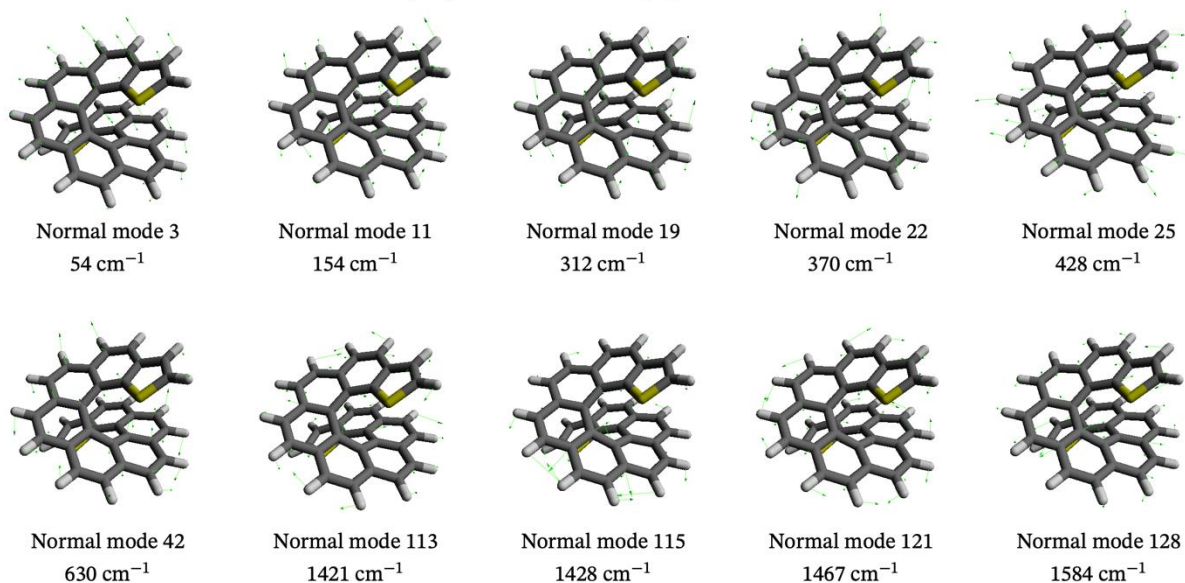


Figure S18 Selected vibrational normal modes for (M)-endo-dithia[9]helicene related to the most intense vibronic peaks in the calculated CPL spectra. The green vectors indicate the direction of the displacement for the corresponding frequency (in cm⁻¹). The numbers refer to the order the normal modes appear in the G16 output.

(M)-exo-dithia[9]helicene

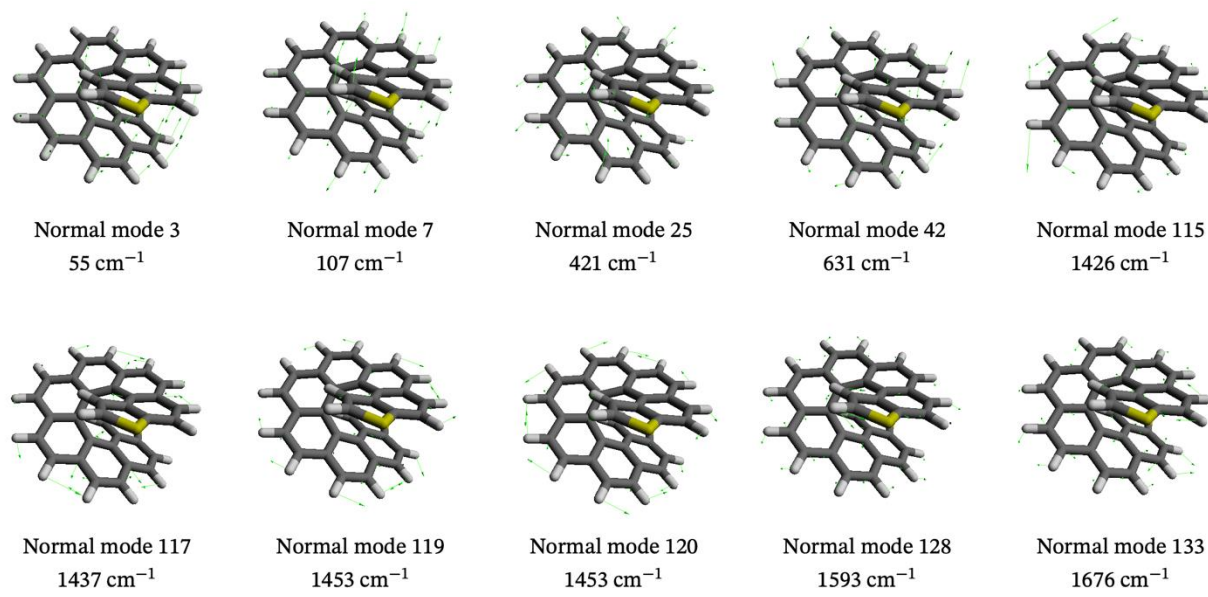


Figure S19 Selected vibrational normal modes for (M)-exo-dithia[9]helicene related to the most intense vibronic peaks in the calculated CPL spectra. The green vectors indicate the direction of the displacement for the corresponding frequency (in cm⁻¹). The numbers refer to the order the normal modes appear in the G16 output.

2. Optimized structures in Cartesian coordinates (xyz format).

(*P*)-endo-dithia[7]helicene, S_0 .

S	0.022427	-0.977779	2.079089
C	-0.619896	-2.461030	2.686901
H	-0.074606	-3.003020	3.459903
C	-1.788297	-2.811961	2.095641
H	-2.352626	-3.714159	2.337761
C	-2.221458	-1.843856	1.127865
C	-3.443396	-1.842831	0.413676
H	-4.127754	-2.689874	0.508340
C	-3.778465	-0.745513	-0.326903
H	-4.748980	-0.690497	-0.827102
C	-2.904462	0.372490	-0.434878
C	-3.384043	1.571254	-1.045337
H	-4.387279	1.570078	-1.479627
C	-2.654755	2.715014	-0.981517
H	-3.065191	3.664582	-1.335155
C	-1.323161	2.698979	-0.466537
C	-0.619763	3.922723	-0.280841
H	-1.124696	4.859746	-0.530157
C	0.620797	3.922565	0.280892
H	1.125990	4.859464	0.530159
C	1.323882	2.698644	0.466599
C	2.655500	2.714339	0.981544
H	3.066184	3.663805	1.335172
C	3.384511	1.570407	1.045310
H	4.387770	1.568978	1.479544
C	2.904616	0.371771	0.434824
C	3.778366	-0.746409	0.326730
H	4.748932	-0.691647	0.826862
C	3.443007	-1.843600	-0.413910
H	4.127142	-2.690816	-0.508633

C	2.221007	-1.844312	-1.127981
C	1.787441	-2.812394	-2.095595
H	2.351511	-3.714753	-2.337726
C	0.619182	-2.461076	-2.686897
H	0.073710	-3.002890	-3.459891
S	-0.022739	-0.977671	-2.079020
C	1.318406	-0.776436	-0.980701
C	1.599917	0.339615	-0.128414
C	0.718490	1.471944	0.100875
C	-0.718110	1.472133	-0.100728
C	-1.599838	0.340035	0.128512
C	-1.318661	-0.776128	0.980774

(*M*)-*exo*-dithia[7]helicene, S_0 .

S	-2.951929	-1.695065	1.999248
C	-1.707859	-2.190401	0.894692
C	-1.730163	-3.376745	0.134322
H	-2.606338	-4.029124	0.141831
C	-0.596269	-3.718651	-0.549446
H	-0.544678	-4.668135	-1.088923
C	0.550600	-2.874762	-0.560192
C	1.762724	-3.354134	-1.146676
H	1.762225	-4.341539	-1.615996
C	2.911566	-2.640262	-1.028168
H	3.865337	-3.048796	-1.372657
C	2.895472	-1.320913	-0.480126
C	4.120866	-0.622363	-0.283488
H	5.057395	-1.126761	-0.535846
C	4.121986	0.614978	0.283588
H	5.059426	1.117669	0.535973
C	2.897858	1.315760	0.480171
C	2.916313	2.635085	1.028203
H	3.870810	3.041895	1.372713

C	1.768761	3.351041	1.146657
H	1.770027	4.338454	1.615953
C	0.555790	2.873852	0.560140
C	-0.589569	3.719798	0.549330
H	-0.536304	4.669188	1.088806
C	-1.724054	3.379888	-0.134447
H	-2.599076	4.033808	-0.141984
C	-1.703869	2.193457	-0.894751
S	-2.948889	1.700176	-1.999157
C	-1.991138	0.359901	-2.522994
H	-2.362839	-0.301790	-3.305129
C	-0.801130	0.272568	-1.877694
H	-0.065984	-0.491906	-2.113651
C	-0.609176	1.313917	-0.897922
C	0.525474	1.597828	-0.061281
C	1.669123	0.715968	0.111762
C	1.667811	-0.718901	-0.111749
C	0.522558	-1.598698	0.061262
C	-0.611588	-1.312820	0.897913
C	-0.801674	-0.271218	1.877786
H	-0.065170	0.491932	2.113788
C	-1.991944	-0.356301	2.522892
H	-2.362555	0.306085	3.304959

(*M*)-*exo*-dithia[7]helicene, S_1 .

S	-2.9476010	-1.6193400	2.0400590
C	-1.7107500	-2.1515770	0.9483820
C	-1.7591800	-3.3294820	0.1795540
H	-2.6474940	-3.9644140	0.1816740
C	-0.6284040	-3.6864750	-0.5201050
H	-0.6045400	-4.6287250	-1.0742830
C	0.5315470	-2.8738820	-0.5305960
C	1.7193170	-3.3353350	-1.1565780

H	1.7073410	-4.3135420	-1.6446220
C	2.8909640	-2.6147930	-1.0789750
H	3.8205480	-3.0294400	-1.4783720
C	2.9189820	-1.3298280	-0.4925470
C	4.1306320	-0.6376000	-0.2883670
H	5.0700180	-1.1331220	-0.5462850
C	4.1329200	0.6228270	0.2885790
H	5.0741020	1.1149570	0.5464460
C	2.9237970	1.3194820	0.4926780
C	2.9004540	2.6046580	1.0788520
H	3.8315380	3.0159920	1.4781840
C	1.7314590	3.3295320	1.1561960
H	1.7230530	4.3078980	1.6439950
C	0.5420390	2.8723010	0.5302460
C	-0.6149260	3.6891400	0.5194510
H	-0.5876300	4.6314690	1.0733390
C	-1.7469790	3.3360770	-0.1801450
H	-2.6329620	3.9742610	-0.1824940
C	-1.7028740	2.1577170	-0.9485380
S	-2.9416570	1.6295850	-2.0400210
C	-1.9618020	0.2998240	-2.5623460
H	-2.3300820	-0.3759290	-3.3338840
C	-0.7644270	0.2426390	-1.9261290
H	-0.0148010	-0.5114240	-2.1535530
C	-0.5854580	1.2942690	-0.9582230
C	0.5401850	1.5851690	-0.1200150
C	1.6628140	0.7114030	0.0842790
C	1.6602170	-0.7172230	-0.0840640
C	0.5343830	-1.5869270	0.1200200
C	-0.5901730	-1.2922320	0.9583860
C	-0.7652200	-0.2404610	1.9268630
H	-0.0127870	0.5106630	2.1547160
C	-1.9627910	-0.2935170	2.5630660

H -2.3285360 0.3831900 3.3349750

(*M*)-endo-dithia[9]helicene, S_0 .

S -2.596477 0.736645 1.350663

C -4.011172 -0.249243 1.456835

H -4.994475 0.220994 1.431960

C -3.727270 -1.570989 1.561880

H -4.481264 -2.355656 1.645576

C -2.313550 -1.825312 1.588930

C -1.670694 -3.064067 1.832001

H -2.265262 -3.977762 1.912753

C -0.321781 -3.080569 2.045883

H 0.183821 -4.010539 2.319144

C 0.457907 -1.890936 1.968736

C 1.810438 -1.906032 2.430674

H 2.239862 -2.857227 2.756152

C 2.502502 -0.745581 2.572386

H 3.491346 -0.734638 3.038495

C 1.970893 0.483352 2.073927

C 2.674324 1.706454 2.279659

H 3.599086 1.685198 2.862606

C 2.160736 2.883078 1.826100

H 2.639531 3.836040 2.066923

C 1.034567 2.885649 0.953174

C 0.531439 4.111962 0.425764

H 0.983891 5.049483 0.759978

C -0.529850 4.112110 -0.426003

H -0.982025 5.049754 -0.760258

C -1.033426 2.885943 -0.953338

C -2.159649 2.883737 -1.826169

H -2.638123 3.836853 -2.066997

C -2.673681 1.707260 -2.279659

H -3.598447 1.686299 -2.862606

C	-1.970694	0.483920	-2.073911
C	-2.502738	-0.744842	-2.572384
H	-3.491554	-0.733491	-3.038532
C	-1.811101	-1.905547	-2.430663
H	-2.240807	-2.856592	-2.756204
C	-0.458556	-1.890919	-1.968713
C	0.320785	-3.080806	-2.045903
H	-0.185134	-4.010579	-2.319234
C	1.669688	-3.064728	-1.831956
H	2.264003	-3.978574	-1.912690
C	2.312898	-1.826137	-1.588834
C	3.726709	-1.572183	-1.561832
H	4.480453	-2.357070	-1.645532
C	4.010921	-0.250500	-1.456794
H	4.994360	0.219480	-1.431956
S	2.596518	0.735789	-1.350577
C	1.548271	-0.656803	-1.444548
C	0.120519	-0.668520	-1.539283
C	-0.742722	0.487980	-1.377358
C	-0.428744	1.660245	-0.584758
C	0.429501	1.660157	0.584610
C	0.742917	0.487855	1.377411
C	-0.120802	-0.668324	1.539366
C	-1.548572	-0.656148	1.444612

(*M*)-endo-dithia[9]helicene, S_1 .

S	2.6144610	0.7588340	-1.3521070
C	4.0335190	-0.2268340	-1.3955320
H	5.0151380	0.2458330	-1.3552400
C	3.7566980	-1.5531670	-1.4776190
H	4.5161960	-2.3356490	-1.5226400
C	2.3468380	-1.8144400	-1.5349620
C	1.7087680	-3.0597140	-1.7512530

H	2.3045720	-3.9748950	-1.7951110
C	0.3582420	-3.0861340	-1.9803550
H	-0.1411030	-4.0269440	-2.2265420
C	-0.4259130	-1.9017440	-1.9451190
C	-1.7820430	-1.9314280	-2.3747160
H	-2.2138570	-2.8903210	-2.6729910
C	-2.5016020	-0.7738850	-2.5114200
H	-3.5054710	-0.7923230	-2.9440790
C	-1.9784000	0.4661180	-2.0658120
C	-2.6913960	1.6741810	-2.2567770
H	-3.6294440	1.6463690	-2.8171560
C	-2.1857320	2.8717480	-1.7942570
H	-2.6922060	3.8134040	-2.0225860
C	-1.0493230	2.8986500	-0.9589660
C	-0.5351050	4.1078480	-0.4397600
H	-0.9777220	5.0511070	-0.7710100
C	0.5317440	4.1085490	0.4379240
H	0.9734060	5.0523660	0.7688610
C	1.0471420	2.9000440	0.9575560
C	2.1834640	2.8744230	1.7929540
H	2.6891960	3.8165690	2.0208850
C	2.6900640	1.6774050	2.2561400
H	3.6281430	1.6506820	2.8165300
C	1.9781560	0.4687130	2.0656440
C	2.5022810	-0.7707640	2.5113760
H	3.5062120	-0.7884870	2.9439330
C	1.7835230	-1.9289720	2.3750640
H	2.2162240	-2.8874090	2.6735230
C	0.4273450	-1.9004780	1.9457530
C	-0.3560260	-3.0853720	1.9813490
H	0.1439570	-4.0258150	2.2276540
C	-1.7066260	-3.0599270	1.7524770
H	-2.3017480	-3.9755300	1.7966500

C	-2.3455750	-1.8151580	1.5359230
C	-3.7555520	-1.5547400	1.4785630
H	-4.5145960	-2.3376440	1.5238740
C	-4.0331990	-0.2285770	1.3960770
H	-5.0151360	0.2434200	1.3556850
S	-2.6147900	0.7579780	1.3520820
C	-1.5756810	-0.6398940	1.4407500
C	-0.1531440	-0.6545610	1.5506320
C	0.7099610	0.4907400	1.3893680
C	0.4127110	1.6473690	0.5863150
C	-0.4139060	1.6467550	-0.5872230
C	-0.7104180	0.4893810	-1.3895890
C	0.1535930	-0.6554100	-1.5503100
C	1.5761760	-0.6396830	-1.4401660

(*P*)-*exo*-dithia[9]helicene, S_0 .

S	-3.956099	-1.470825	-1.409333
C	-2.238556	-1.711280	-1.505148
C	-1.606585	-2.948871	-1.744316
H	-2.186700	-3.873434	-1.789206
C	-0.262404	-2.941719	-1.995764
H	0.251502	-3.868428	-2.264458
C	0.498856	-1.738827	-1.948974
C	1.850544	-1.745851	-2.414351
H	2.288653	-2.694783	-2.734790
C	2.534627	-0.581200	-2.556295
H	3.525216	-0.564214	-3.018393
C	1.993927	0.644193	-2.059237
C	2.696570	1.868640	-2.259030
H	3.624508	1.849957	-2.836927
C	2.180253	3.042976	-1.803669
H	2.658849	3.997477	-2.038693
C	1.046215	3.041057	-0.939667

C	0.535623	4.268567	-0.418898
H	0.991605	5.205997	-0.748528
C	-0.536062	4.268520	0.418823
H	-0.992162	5.205907	0.748396
C	-1.046524	3.040970	0.939635
C	-2.180564	3.042784	1.803602
H	-2.659313	3.997221	2.038575
C	-2.696720	1.868403	2.259054
H	-3.624634	1.849668	2.836996
C	-1.993943	0.644053	2.059297
C	-2.534540	-0.581396	2.556348
H	-3.525142	-0.564488	3.018426
C	-1.850392	-1.745997	2.414389
H	-2.288459	-2.694970	2.734771
C	-0.498710	-1.738857	1.948985
C	0.262631	-2.941695	1.995696
H	-0.251206	-3.868470	2.264319
C	1.606802	-2.948772	1.744194
H	2.186926	-3.873338	1.788966
C	2.238709	-1.711139	1.505101
S	3.956232	-1.470539	1.409320
C	3.739819	0.243364	1.327088
H	4.608189	0.900020	1.277748
C	2.435423	0.614365	1.340974
H	2.124011	1.655834	1.326449
C	1.527589	-0.504582	1.417805
C	0.094125	-0.521009	1.530333
C	-0.760422	0.643088	1.370310
C	-0.437768	1.814950	0.579528
C	0.437672	1.814986	-0.579476
C	0.760417	0.643112	-1.370263
C	-0.094066	-0.521015	-1.530296
C	-1.527536	-0.504674	-1.417775

C	-2.435452	0.614187	-1.340908
H	-2.124151	1.655681	-1.326328
C	-3.739828	0.243078	-1.327015
H	-4.608200	0.899720	-1.277592

(*P*)-*exo*-dithia[9]helicene, S_1 .

S	-3.9714570	-1.4472340	-1.3476280
C	-2.2566110	-1.6972110	-1.4682000
C	-1.6288630	-2.9403940	-1.6727340
H	-2.2096490	-3.8652670	-1.6866550
C	-0.2792450	-2.9443670	-1.9266200
H	0.2304480	-3.8822320	-2.1626750
C	0.4853090	-1.7490990	-1.9140130
C	1.8479630	-1.7731430	-2.3290750
H	2.2908480	-2.7311100	-2.6139480
C	2.5635920	-0.6137360	-2.4573350
H	3.5758990	-0.6289420	-2.8698220
C	2.0270440	0.6253420	-2.0226880
C	2.7435660	1.8334330	-2.1991450
H	3.6918420	1.8065660	-2.7419100
C	2.2290260	3.0293790	-1.7425180
H	2.7375700	3.9725940	-1.9596950
C	1.0749430	3.0521750	-0.9299290
C	0.5453030	4.2611460	-0.4242280
H	0.9949470	5.2052410	-0.7436590
C	-0.5461620	4.2611700	0.4232050
H	-0.9959820	5.2052710	0.7423600
C	-1.0755130	3.0522500	0.9293300
C	-2.2294680	3.0294930	1.7421030
H	-2.7381280	3.9726870	1.9591070
C	-2.7437250	1.8335960	2.1991690
H	-3.6919400	1.8067480	2.7420480
C	-2.0270450	0.6255700	2.0229230

C	-2.5633580	-0.6134900	2.4578630
H	-3.5756020	-0.6287830	2.8705120
C	-1.8476250	-1.7728490	2.3296520
H	-2.2904070	-2.7308160	2.6146970
C	-0.4850340	-1.7487200	1.9143930
C	0.2796570	-2.9438920	1.9270150
H	-0.2299010	-3.8818060	2.1631670
C	1.6292500	-2.9397930	1.6729950
H	2.2101170	-3.8646160	1.6868740
C	2.2568510	-1.6965630	1.4683200
S	3.9716540	-1.4464010	1.3474620
C	3.7488440	0.2698570	1.3126450
H	4.6147660	0.9296320	1.2624190
C	2.4435490	0.6365260	1.3616110
H	2.1264580	1.6767530	1.3735320
C	1.5417810	-0.4851190	1.4259220
C	0.1108860	-0.5063090	1.5398150
C	-0.7439930	0.6443330	1.3715260
C	-0.4295300	1.8012470	0.5749350
C	0.4291290	1.8011710	-0.5752520
C	0.7439090	0.6440570	-1.3714680
C	-0.1107890	-0.5067160	-1.5396210
C	-1.5416980	-0.4856800	-1.4258520
C	-2.4435870	0.6358600	-1.3616010
H	-2.1266270	1.6761250	-1.3734550
C	-3.7488530	0.2690380	-1.3127560
H	-4.6148220	0.9287510	-1.2625600

3. Additional structures optimized with ω B97X-D/def2-SV(P).

(*M*)-*exo*-dithia[7]helicene, S_0 .

S	-3.0001210	-1.4270700	1.9286820
C	-1.7296070	-2.0378780	0.9151940
C	-1.7707830	-3.2542670	0.2008810
H	-2.6756520	-3.8671780	0.1902590
C	-0.6208520	-3.6767840	-0.4117790
H	-0.5895110	-4.6520580	-0.9064020
C	0.5590660	-2.8767710	-0.4152520
C	1.7763310	-3.4087070	-0.9477580
H	1.7694650	-4.4201740	-1.3645530
C	2.9372140	-2.7065030	-0.8490840
H	3.8885030	-3.1510520	-1.1560060
C	2.9327470	-1.3528230	-0.3862420
C	4.1586990	-0.6397550	-0.2375710
H	5.0979200	-1.1582050	-0.4516410
C	4.1589190	0.6383750	0.2377700
H	5.0983130	1.1564710	0.4519470
C	2.9332110	1.3518830	0.3863050
C	2.9381000	2.7055900	0.8490630
H	3.8895170	3.1498240	1.1560310
C	1.7774880	3.4082430	0.9475670
H	1.7709830	4.4197310	1.3643090
C	0.5600550	2.8767360	0.4150350
C	-0.6195980	3.6771380	0.4115050
H	-0.5879650	4.6524330	0.9060610
C	-1.7696810	3.2549310	-0.2010590
H	-2.6743790	3.8680890	-0.1903590
C	-1.7289420	2.0384740	-0.9152690
S	-2.9998510	1.4277750	-1.9283260
C	-1.9965420	0.1193550	-2.4505760
H	-2.3711900	-0.5944650	-3.1847640

C	-0.7694390	0.1262300	-1.8692510
H	-0.0018900	-0.6048650	-2.1147310
C	-0.5923900	1.2150680	-0.9401190
C	0.5513130	1.5750470	-0.1483610
C	1.7079630	0.7220000	0.0628890
C	1.7077050	-0.7225150	-0.0629070
C	0.5507590	-1.5751370	0.1482490
C	-0.5927890	-1.2148550	0.9400500
C	-0.7693790	-0.1260880	1.8693560
H	-0.0015600	0.6047560	2.1147520
C	-1.9965640	-0.1186460	2.4504960
H	-2.3710180	0.5953490	3.1846150

(*M*)-*exo*-dithia[7]helicene, S_1 .

S	-3.0097380	1.2258080	-1.9294310
C	-1.7398670	1.9233820	-0.9767960
C	-1.8134600	3.1438690	-0.2750750
H	-2.7406260	3.7212290	-0.2489690
C	-0.6619080	3.6191450	0.3166380
H	-0.6655760	4.5979080	0.8056760
C	0.5433240	2.8721260	0.3115480
C	1.7409630	3.4142910	0.8526200
H	1.7206950	4.4293600	1.2602840
C	2.9293310	2.7130400	0.8049420
H	3.8575460	3.1817640	1.1453590
C	2.9700620	1.3747630	0.3476240
C	4.1817600	0.6600700	0.2153040
H	5.1248100	1.1772940	0.4138480
C	4.1817570	-0.6600600	-0.2153260
H	5.1248060	-1.1772810	-0.4138850
C	2.9700600	-1.3747600	-0.3476350
C	2.9293370	-2.7130350	-0.8049500
H	3.8575530	-3.1817620	-1.1453650

C	1.7409650	-3.4142900	-0.8526150
H	1.7207040	-4.4293630	-1.2602720
C	0.5433310	-2.8721240	-0.3115430
C	-0.6618990	-3.6191450	-0.3166320
H	-0.6655680	-4.5979040	-0.8056800
C	-1.8134560	-3.1438710	0.2750830
H	-2.7406240	-3.7212310	0.2489630
C	-1.7398580	-1.9233880	0.9768060
S	-3.0097370	-1.2257940	1.9294050
C	-1.9658280	0.0558630	2.4508690
H	-2.3351360	0.8070030	3.1495650
C	-0.7209780	-0.0241070	1.9127640
H	0.0727680	0.6812100	2.1543770
C	-0.5648050	-1.1438710	1.0211670
C	0.5726380	-1.5459260	0.2497750
C	1.7156690	-0.7175920	-0.0110490
C	1.7156760	0.7175990	0.0110430
C	0.5726370	1.5459430	-0.2497770
C	-0.5648160	1.1438690	-1.0211660
C	-0.7209960	0.0240910	-1.9127460
H	0.0727370	-0.6812400	-2.1543510
C	-1.9658640	-0.0559050	-2.4508100
H	-2.3351670	-0.8070690	-3.1494810

Section S3: Additional references.

-
- ¹ Wender, P.A.; Lesser, A.B.; Sirois, L.E. *Angew. Chem.* **2012**, *124*, 2790-2794.
- ² Dipold, J.; Batista, R.J.M.B.; Fonseca, R.D.; Silva, D.L.; Moura, G.L.C.; dos Anjos, J.V.; Simas, A.M.; De Boni, L.; Mendonca, C.R. *Chem. Phys. Lett.* **2016**, *661*, 143-150.
- ³ Lang, J.; Jie, L.; Yanjun, S.; Xiaosong, S. CN113754629A, **2021**
- ⁴ Lee, J.-E.; Kwon, J.; Yun, J. *Chem. Commun.* **2008**, 733-734
- ⁵ Molloy, J.J.; Seath, C.P.; West, M.J.; McLaughlin, C.; Fazakerley, N.J.; Kennedy, A.R.; Nelson, D.J.; Watson, A.J.B. *J. Am. Chem. Soc.* **2018**, *140*, 1, 126-130.
- ⁶ G. A. Molander and A. R. Brawn, *J. Org. Chem.*, 2006, **71**, 9681-9686.
- ⁷ Yanai, T.; Tew, D. P.; Handy, N. C. *Chem. Phys. Lett.* 2004, 393, 51–57.
- ⁸ Weigend, F.; Ahlrichs, R. *Phys. Chem. Chem. Phys.* 2005, 7, 3295–3305.
- ⁹ Frisch, M. J.; Trucks, G. W.; Schlegel, H. B.; Scuseria, G. E.; Robb, M. A.; Cheeseman, J. R.; Scalmani, G.; Barone, V.; Petersson, G. A.; Nakatsuji, H.; Li, X.; Caricato, M.; Marenich, A. V.; Bloino, J.; Janesko, B. G.; Gomperts, R.; Mennucci, B.; Hratchian, H. P.; Ortiz, J. V.; Izmaylov, A. F.; Sonnenberg, J. L.; Williams-Young, D.; Ding, F.; Lipparini, F.; Egidi, F.; Goings, J.; Peng, B.; Petrone, A.; Henderson, T.; Ranasinghe, D.; Zakrzewski, V. G.; Gao, J.; Rega, N.; Zheng, G.; Liang, W.; Hada, M.; Ehara, M.; Toyota, K.; Fukuda, R.; Hasegawa, J.; Ishida, M.; Nakajima, T.; Honda, Y.; Kitao, O.; Nakai, H.; Vreven, T.; Throssell, K.; Montgomery, J. A., Jr.; Peralta, J. E.; Ogliaro, F.; Bearpark, M. J.; Heyd, J. J.; Brothers, E. N.; Kudin, K. N.; Staroverov, V. N.; Keith, T. A.; Kobayashi, R.; Normand, J.; Raghavachari, K.; Rendell, A. P.; Burant, J. C.; Iyengar, S. S.; Tomasi, J.; Cossi, M.; Millam, J. M.; Klene, M.; Adamo, C.; Cammi, R.; Ochterski, J. W.; Martin, R. L.; Morokuma, K.; Farkas, O.; Foresman, J. B.; Fox, D. J. *Gaussian 16 Revision c.01*.
- ¹⁰ Santoro, F.; Lami, A.; Improta, R.; Bloino, J.; Barone, V. *J. Chem. Phys.* 2008, *128* (22), 224311–224317.
- ¹¹ Srebro-Hooper, M.; Autschbach, J. *Annu. Rev. Phys. Chem.* 2017, *68*, 399–420.
- ¹² Autschbach, J.; Nitsch-Velasquez, L.; Rudolph, M. *Top. Curr. Chem.* 2011, *298*, 1–98.
- ¹³ Zhao, Y.; Truhlar, D. G. *Acc. Chem. Res.* 2008, *41* (2), 157–167.
- ¹⁴ Peverati, R.; Truhlar, D. G. *J. Phys. Chem. Lett.* 2011, *2*, 2810–2817.
- ¹⁵ Chai, J.-D.; Head-Gordon, M. *Phys. Chem. Chem. Phys.* 2008, *10* (44), 6615.
- ¹⁶ Henderson, T. M.; Izmaylov, A. F.; Scalmani, G.; Scuseria, G. E. *J. Chem. Phys.* 2009, *131* (4), 044108.
- ¹⁷ Migliore, A. J. *Chem. Theory Comput.* 2019, *15* (9), 4915–4923.
- ¹⁸ Liu, Y.; Cerezo, J.; Mazzeo, G.; Lin, N.; Zhao, X.; Longhi, G.; Abbate, S.; Santoro, F. J. *Chem. Theory Comput.* 2016, *12* (6), 2799–2819.